Theoretical modeling of nanostructures

Yia-Chung Chang (張亞中)

Research Center for Applied Sciences (RCAS)

Academia Sinica, Taiwan

(中研院 應用科學中心)

in collaboration with:

S. Sun, G. Qian (UIUC)

Ming-Ting Kuo (郭明庭),NCU

David Ting, JPL, Caltech

Applications of nanostructure devices

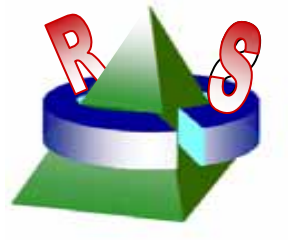

- Single-electron transistor (SET)
- Single-photon generator (SPG)
- Light-emitting transistor
- Optical signal control (slow light)
- Photonic crystals
- QD lasers & detectors
- Non-linear optical devices
- Biosensors
- Spintronics devices

Theoretical approaches

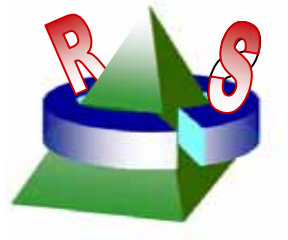

- Envelope Function approximation
- k.p theory
- Effective-mass model (for spherical conduction Band)
- Luttinger model (for degenerate valence bands)
- Effective bond-orbital model
- VFF model (for strain distribution)
- Tight-binding model
- Density-functional theory (DFT)

Well, Wire and Dot

- Well (2d)

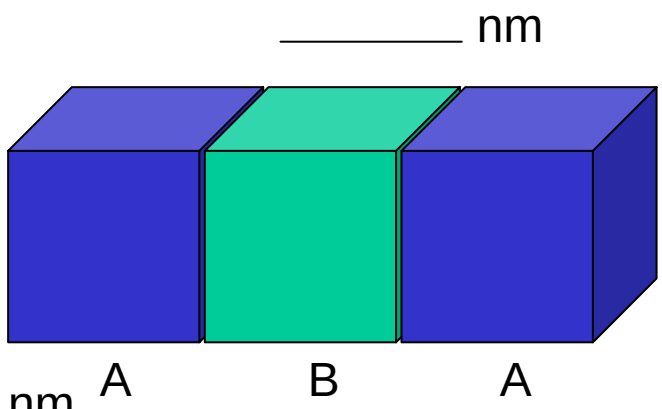

- Wire
(1d)

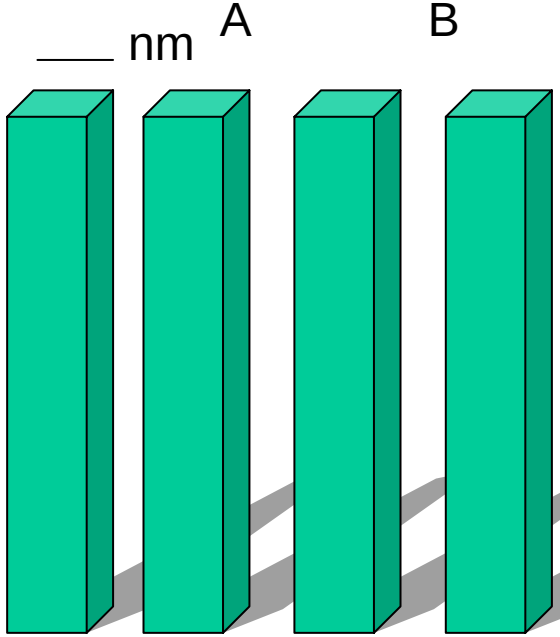

Dot

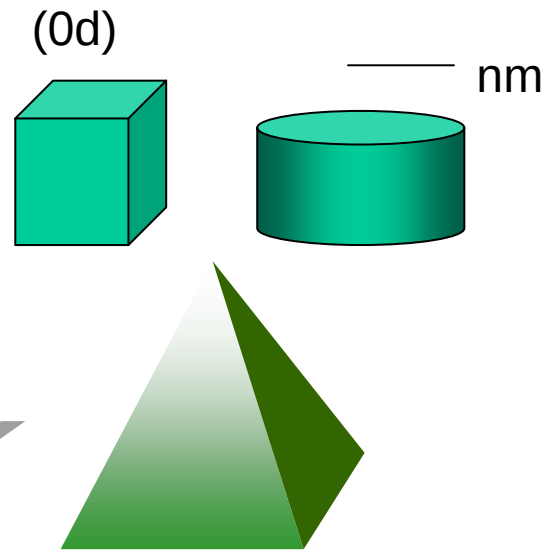

Envelope Function Approximation

(Single electron picture)

- Quantum wells

$$\psi(r) = \varsigma_n(z) e^{i(k_x x + k_y y)} u_b(k \approx 0, r)$$

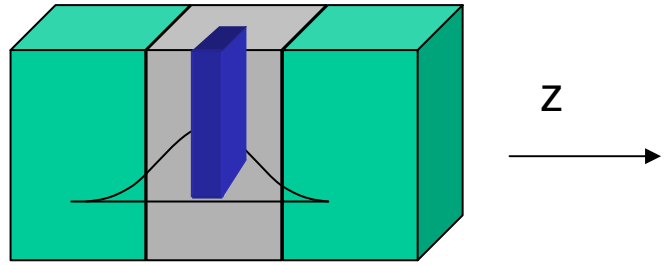

- Quantum wires

$$\psi(r) = \varsigma_n(x)\varsigma(y) e^{ik_z z} u_b(k \approx 0, r)$$

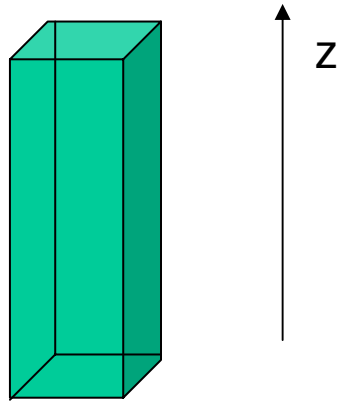

- Quantum dots

$$\psi(r) = \varsigma_n(x)\varsigma_m(y)\varsigma_p(z) u_b(k \approx 0, r)$$

$$\downarrow$$

$$\varsigma_{n,m,l}(x, y, z)$$

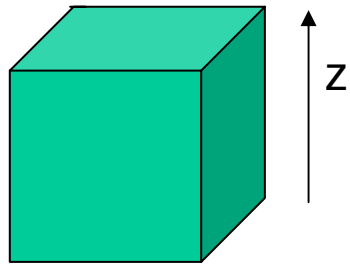

Physical effects in QD

Quantum confinement (size effect)

Selection rule (light polarization)

Discrete energy levels (0-d density of states)

Strong Coulomb interaction (Coulomb blockade)

Strong electron correlation (many-body effect)

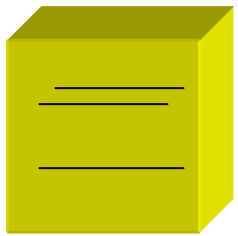

Artificial atom

Self assembled quantum dots

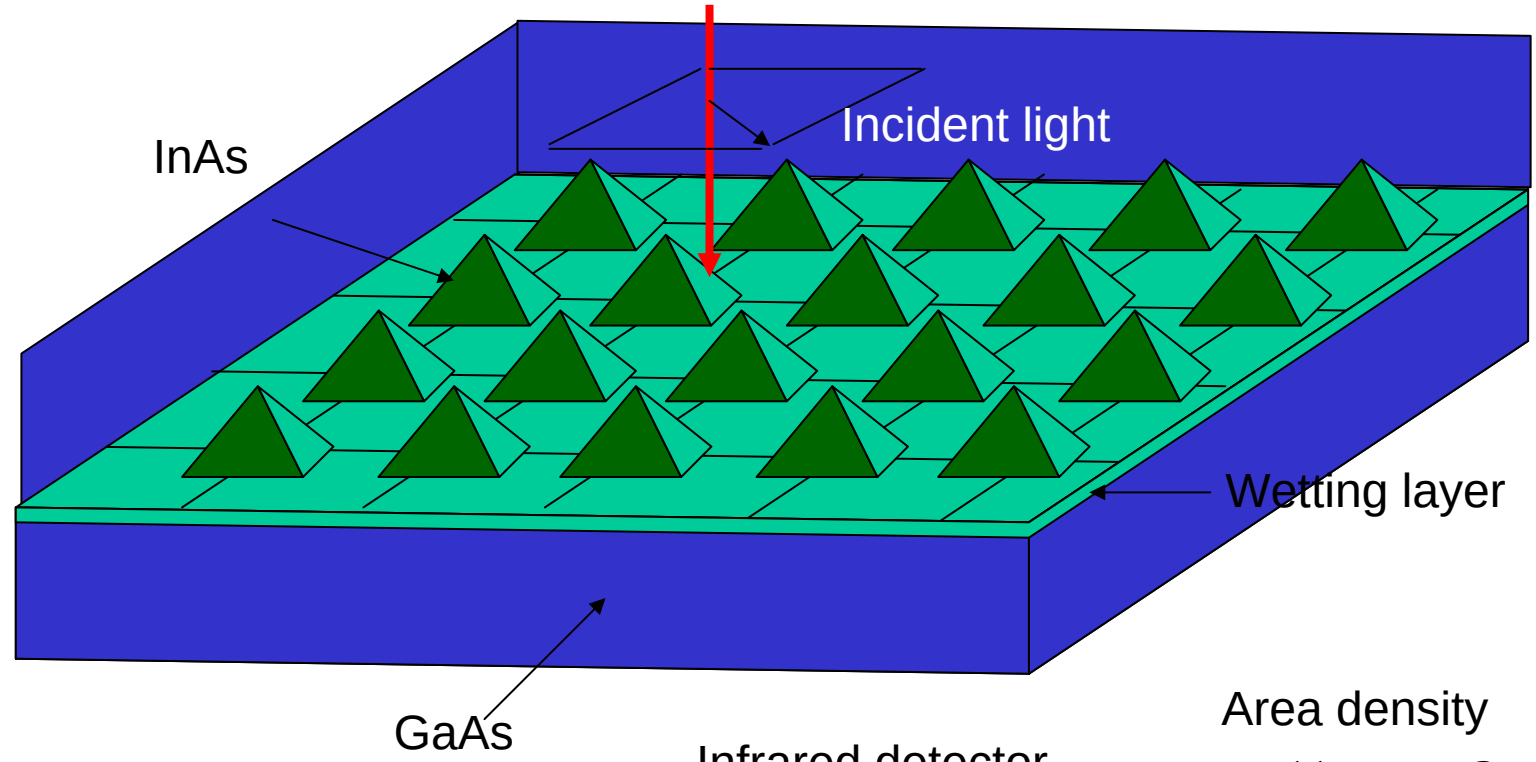

Lattice mismatch 7%

Infrared detector
Laser

Area density

$10^{11} / cm^2$

Theoretical Analysis

- Energy and wave functions computed using a stabilized transfer matrix technique by dividing the system into many slices along growth direction.
- Envelope function approximation with energy-dependent effective mass is used.
- Effective-mass Hamiltonian in k-sapce:

$$[(k_x^2+k_y^2)/m_t(E)+\partial_z^2/m_l(E)-E]F(\mathbf{k}) + \Sigma_{\mathbf{k}'}[V(\mathbf{k},\mathbf{k}')+V_{imp}(\mathbf{k},\mathbf{k}')]F(\mathbf{k}')=0$$

  is solved via plane-wave expansion in each slice.
- 14-band k·p effects included perturbatively in optical matrix elements calculation
- Dopant effects can be incorporated as screened Coulomb potential
- The technique applies to quantum wells and quantum dots (or any 2D periodic nanostructures)

Charge densities of low-lying states in lens-shaped QD

s-like

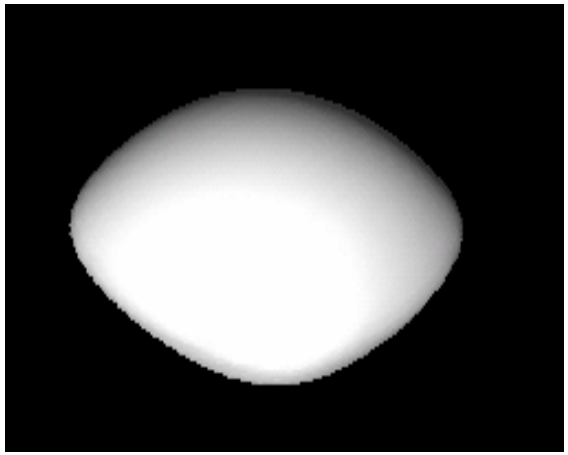

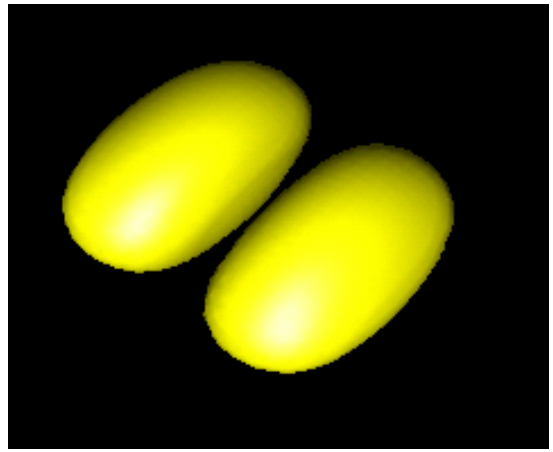

p_x/p_y like

d-like

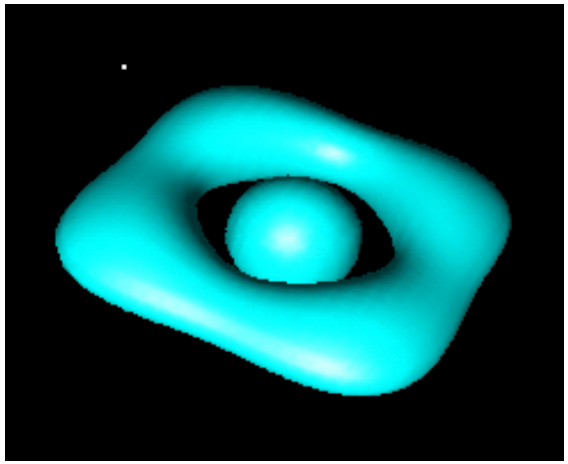

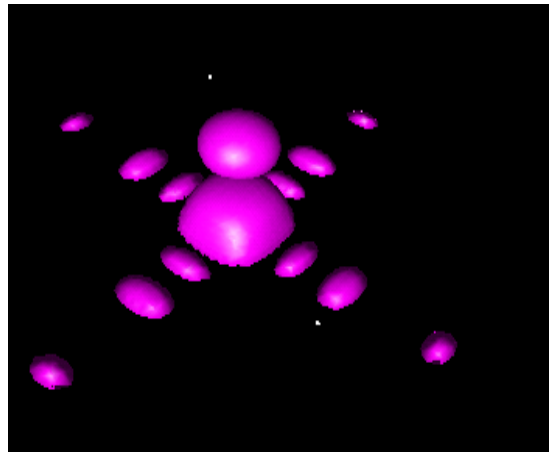

p_z like

Kohn-Luttinger Hamiltonian

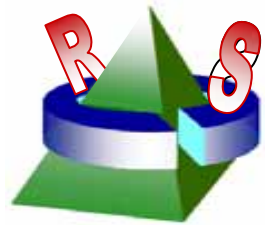

B. Degenerate case: [e.g. valence bands of semiconudctors]

Let $|u_\nu(0)>$ denote the J-fold degenerate states at the zone center (Γ point). Ignore the interactions among $|u_\nu(0)>$'s first. The first-order correction to the perturbed state due coupling to other states is given by

$$|u_\nu(\mathbf{k})>=|u_\nu(0)>+\sum_{n'\neq J}\frac{<u_\nu(0)|\frac{\hbar}{m}\mathbf{k}\cdot\mathbf{p}\,|u_{n'}(0)>}{E_\nu(0)-E_{n'}(0)}|u_{n'}(0)>\,.$$

Thus, the first-order correction to the energy for states $|u_\nu>$'s are given by diagonalizing the perturbed matrix within the J-fold basis (degenerate perturbation theory)

$$H^{(1)}_{\nu\nu'}\equiv E_\nu(0)\delta_{\nu,\nu'}+\sum_{n'\neq J}\frac{<u_\nu(0)|\frac{\hbar}{m}\mathbf{k}\cdot\mathbf{p}|u_{n'}(0)><u_{n'}(0)|\frac{\hbar}{m}\mathbf{k}\cdot\mathbf{p}|u_{\nu'}(0)>}{E_\nu(0)-E_{n'}(0)}.$$

For cubic crystals with p-like valence bands (e.g. Si, Ge, GaAs, InAs,...), we have

$$H^{(1)}=\begin{pmatrix} Ak_x^2+B(k_y^2+k_z^2) & Ck_xk_y & Ck_xk_z \\ - & Ak_y^2+B(k_x^2+k_z^2) & Ck_xk_z \\ - & - & Ak_z^2+B(k_y^2+k_x^2)\end{pmatrix},$$

where A, B, C are three band parameters, which are determined experimentally (typically via cyclotron resonance measurements).

With spin-orbit interaction:

The valence bands become 6-fold, since $J = 1 \bigoplus 1/2 = 1/2, 3/2$. The top four valence bands are given by $|3/2, 3/2> = -\frac{1}{\sqrt{2}}(|x> + i|y>)\uparrow$, $|3/2, 1/2> = -\frac{1}{\sqrt{6}}(|x> + i|y>)\downarrow -2|z>\uparrow$, $|3/2, -1/2> = \frac{1}{\sqrt{6}}(|x> - i|y>)\uparrow +2|z>\downarrow$, $|3/2, -3/2> = \frac{1}{\sqrt{2}}(|x> - i|y>)\downarrow$.

$$H^{(off)} = \frac{\hbar^2}{2m}\begin{pmatrix} A_+ & L & M & 0 \\ L^* & A_- & 0 & M \\ M^* & 0 & A_- & -L \\ 0 & M^* & -L^* & A_+ \end{pmatrix},$$

where

$$A_\pm \equiv (\gamma_1 \pm \gamma_2)(k_x^2 + k_y^2) + (\gamma_1 \mp 2\gamma_2)k_z^2,$$

$$L = -2i\sqrt{3}\gamma_3 K^- k_z, \qquad M = -\sqrt{3}\bar{\gamma}K^{-2} + (\gamma_2 - \gamma_3)k_x k_y$$

$$K^\pm \equiv (k_x \pm ik_y),$$

and

$$\bar{\gamma} = (\gamma_2 + \gamma_3)/2.$$

$\gamma_1, \gamma_2, \gamma_3$ are called "Luttinger parameters" and they are related to A, B, C by $\gamma_1 = \frac{1}{3}(A + B)$, $\gamma_2 = \frac{1}{6}(A - B)$, and $\gamma_3 = \frac{1}{6}C$.

Optical and Structural Characterization of QDIPs

TEM GaAs

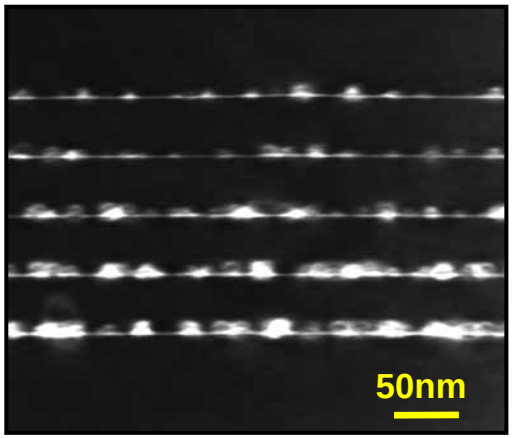

Energies of transitions (from PL/PLE data):
65meV, 89meV
139meV, 195meV

TEM AlGaAs

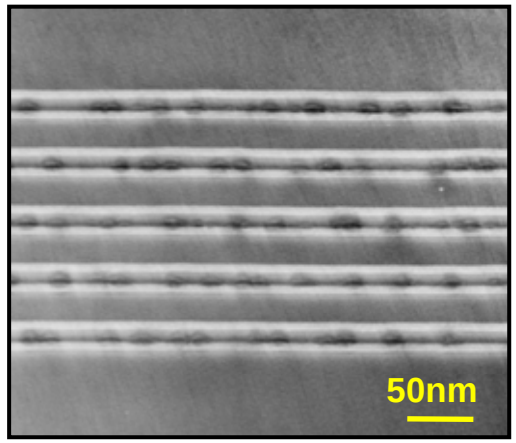

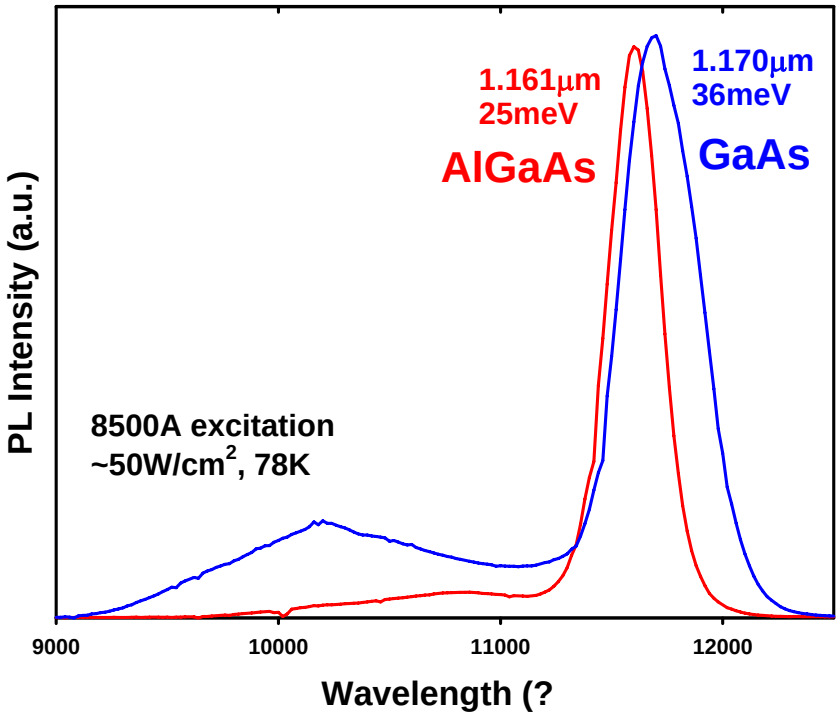

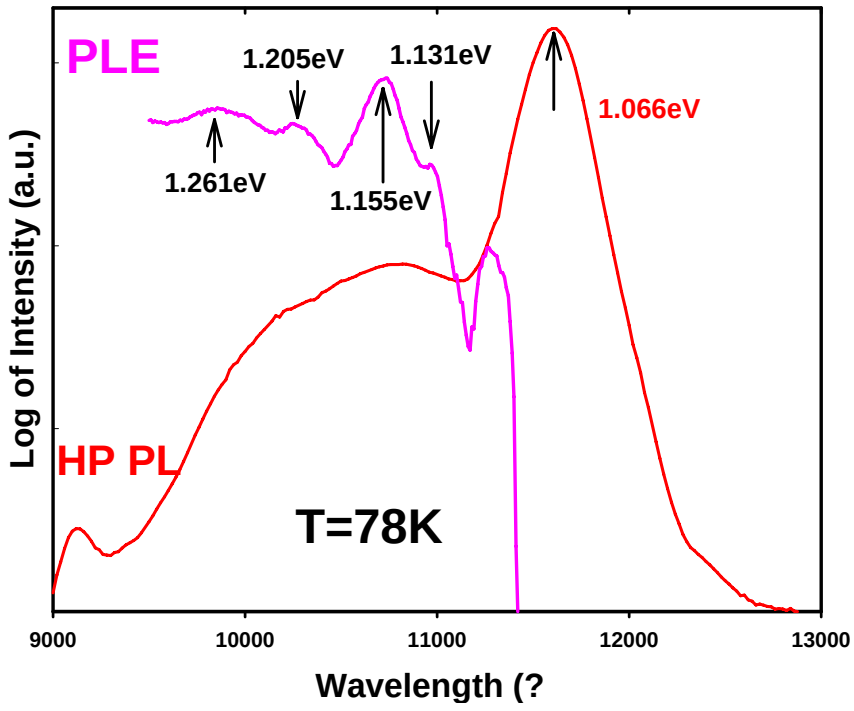

Microscopic modeling

[S. Sun,Y. C. Chang, PRB 62, 13631 (2000)]

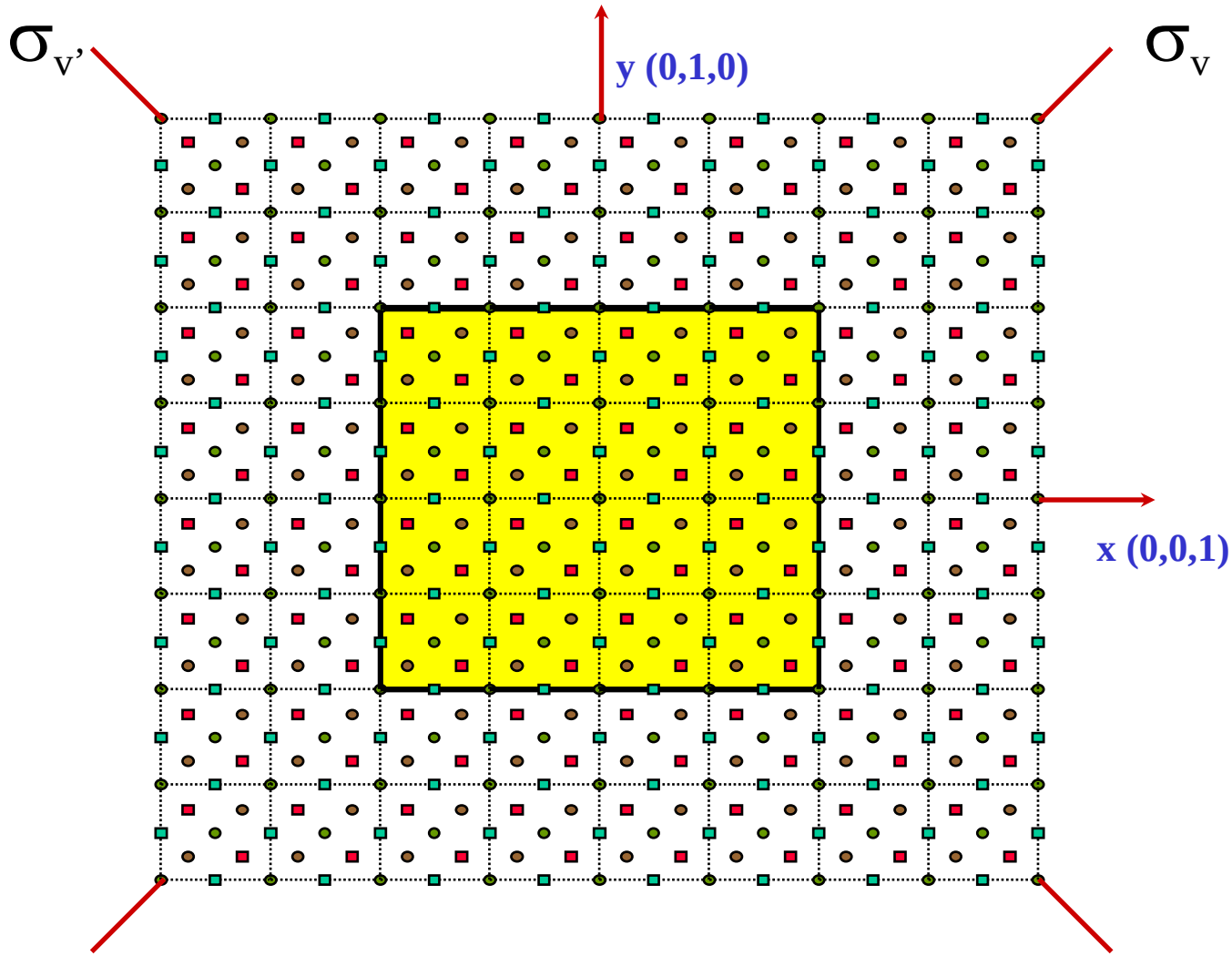

Valence force field (VFF) Model

$$V = \frac{1}{4}\sum_{ij}\frac{3}{4}\alpha_{ij}\left(d_{ij}^2 - d_{0,ij}^2\right)^2 \Big/ d_{0,ij}^2$$

$$+\frac{1}{4}\sum_{i}\sum_{j\neq k}\frac{3}{4}\beta_{ijk}\left(\vec{d}_{ij}\cdot\vec{d}_{ik} + d_{0,ij}d_{0,ik}/3\right)^2 \Big/ d_{0,ij}d_{0,ik}$$

i labels atom positions
j , k label nearest-neighbors of i
d_{ij} = bond length joining sites i and j
$d_{0,ij}$ is the corresponding equilibrium length
α_{ij}= bond stretching constants
d_{ijk}= bond bending constants
We take $d_{ijk}^2 = d_{ij}d_{ik}$

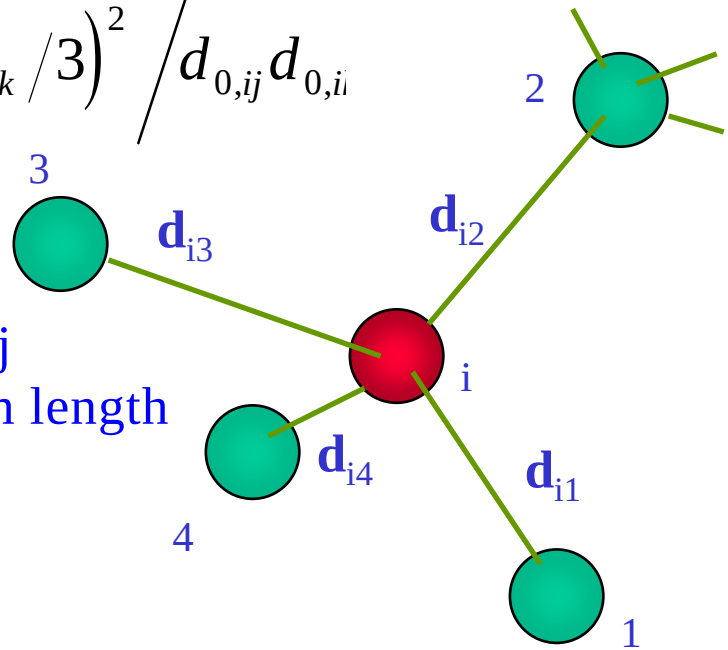

Effective bond-orbital Model
[Y.C.Chang, PRB 37, 8215 (1988)]

$$H_{\alpha,\alpha'}(\vec{k}) = E_p \delta_{\alpha,\alpha'} +$$
$$\sum_{\tau} e^{i\vec{k}\cdot\vec{\tau}} \left\{ E_{xy} \tau_\alpha \tau_{\alpha'} + \left[\left(E_{xx} - E_{xy} \right) \tau_\alpha^2 + E_{zz} \left(1 - \tau_\alpha^2 \right) \right] \delta_{\alpha,\alpha} \right.$$

Strain Hamiltonian

$$H_{st} = \begin{pmatrix} -\Delta V_H + D_1 & \sqrt{3} d e_{xy} & \sqrt{3} d e_{xz} \\ \sqrt{3} d e_{xy} & -\Delta V_H + D_2 & \sqrt{3} d e_{yz} \\ \sqrt{3} d e_{xz} & \sqrt{3} d e_{yz} & -\Delta V_H + D_3 \end{pmatrix}$$

$e_{ij} = (\varepsilon_{ij} + \varepsilon_{ji})/2$
$\Delta V_H = (a_1 + a_2)(\varepsilon_{xx} + \varepsilon_{yy} + \varepsilon_{zz})$
$D_1 = b(2\varepsilon_{xx} - \varepsilon_{yy} - \varepsilon_{zz})$
$D_2 = b(2\varepsilon_{yy} - \varepsilon_{xx} - \varepsilon_{zz})$
$D_3 = b(2\varepsilon_{zz} - \varepsilon_{xx} - \varepsilon_{yy})$
a_1, a_2, b, d = deformation potentials.

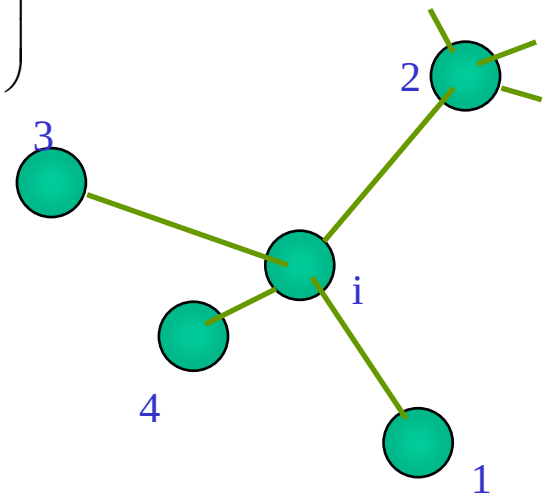

Strain Potential Along Line A and B of Dot 1

UNIVERSITY OF ILLINOIS AT URBANA-CHAMPAIGN

- **Fig.(a):** strain potential along line A
- **Fig.(b):** strain potential along line B

V_{ss}
V_{xx}
V_{yy}
V_{zz}

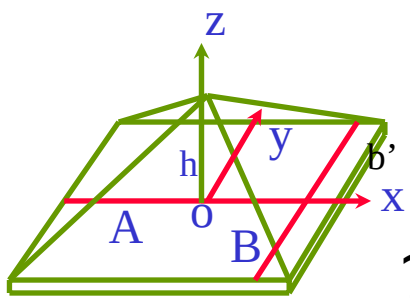

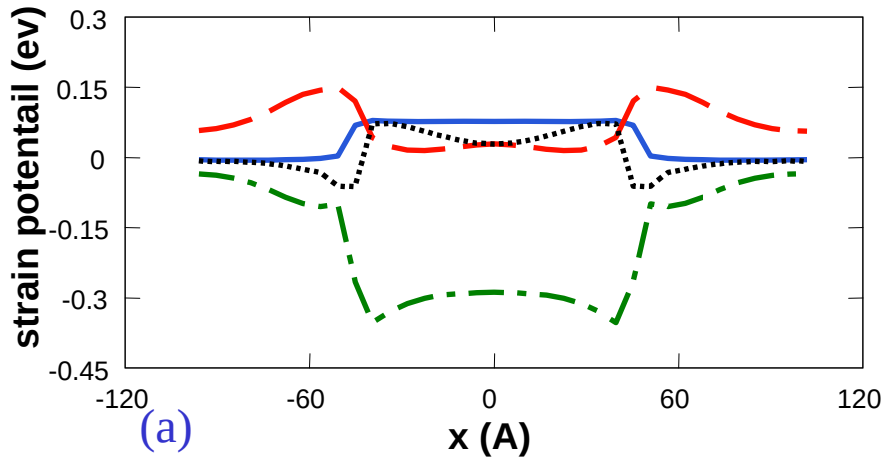

(a)

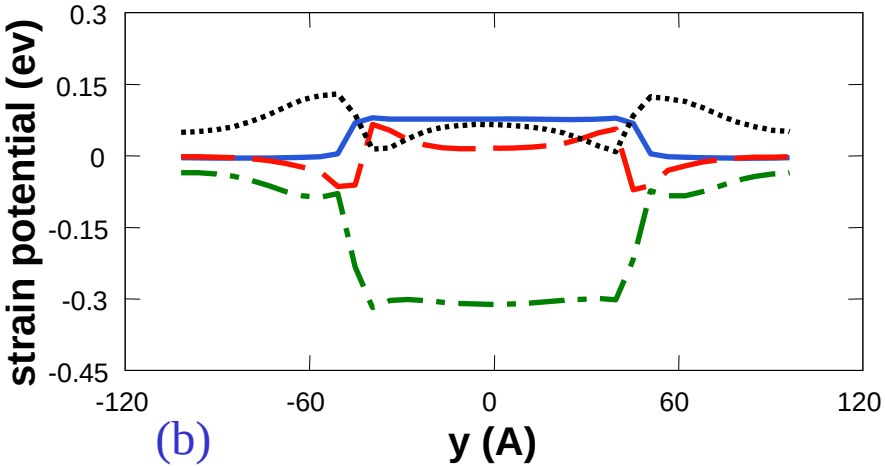

(b)

- **Band offset:**
  CB: 0.833eV
  VB: 0.260eV

Strain Distribution Along [001] of Dot 1 and Dot 2

- **Hydrostatic Strain :**
  - **Dot 1:** ——————
  - **Dot 2:** ....
- **Biaxial Strain:**
  - **Dot 1:** - - - - - -
  - **Dot 2:** — · — · —
- **[001] is growth direction**
- **Dot 1: 0-62.5 A**
  Dot 2: 0-50A

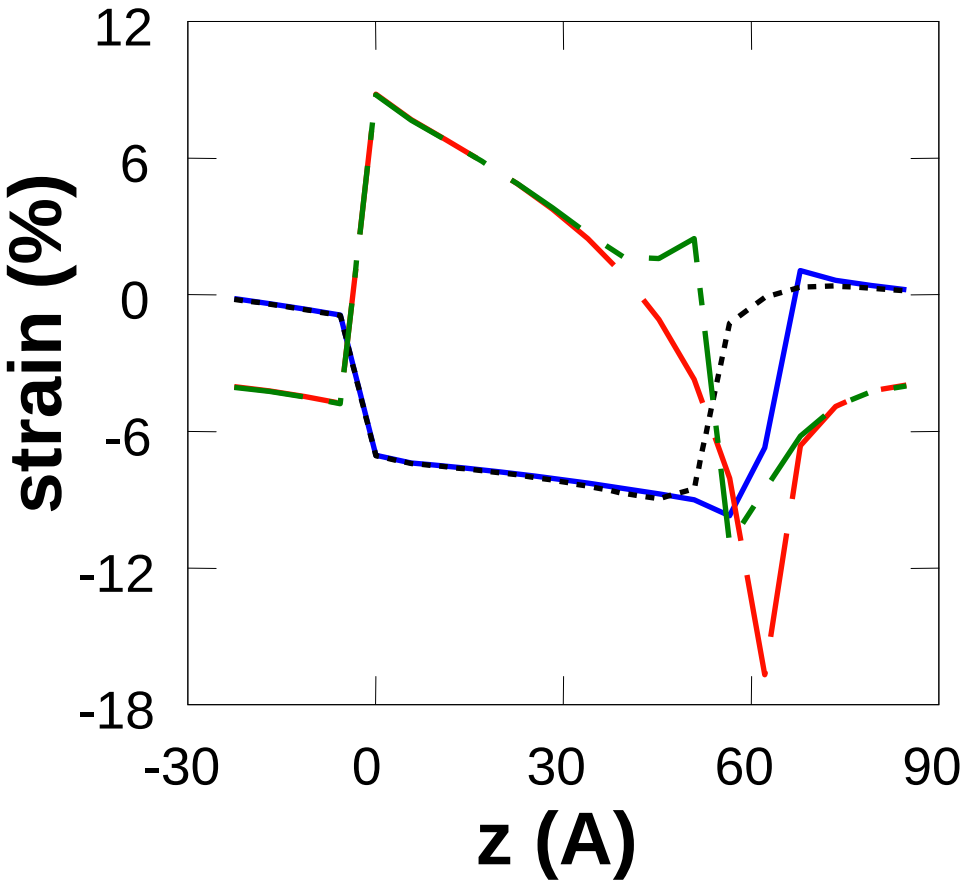

Parameters Used in Calculation

Parameters used in the calculation

Parameters	GaAs	InAs
CB minimum	1.495	0.662
VB maximum (eV)	0.	0.260
spin-orbital coupling (eV)	0.34	0.38
Deformation potentials (eV)		
a_c	-7.17	-5.45
a_v	-2.7	-1.8
b	-1.7	-1.0
d	-5.3	-3.6

Ground Transition Energy Varying With Dot Height (comparing to Experiment)

Dot base length 200Å

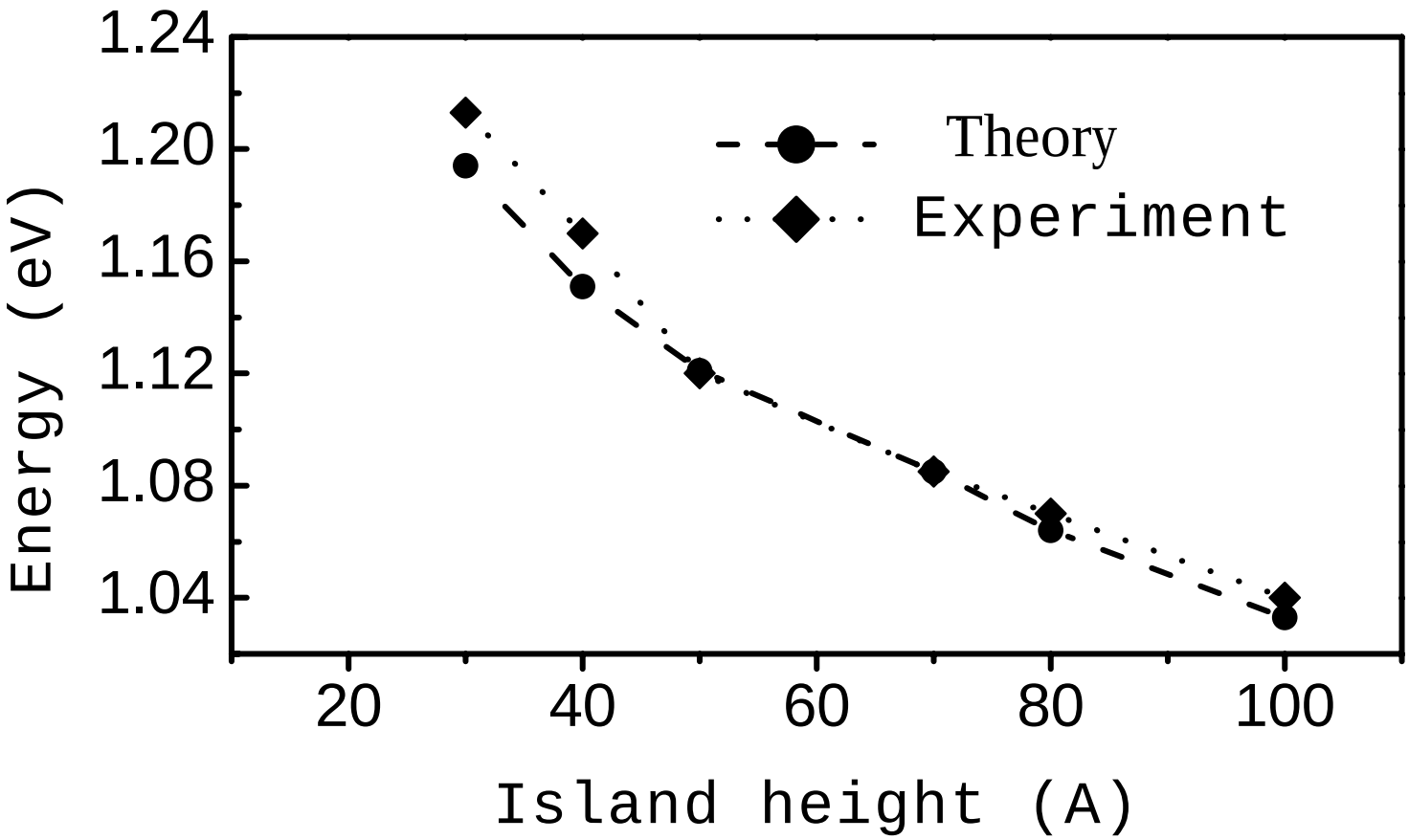

PL/PLE Characterization: Electronic Structure

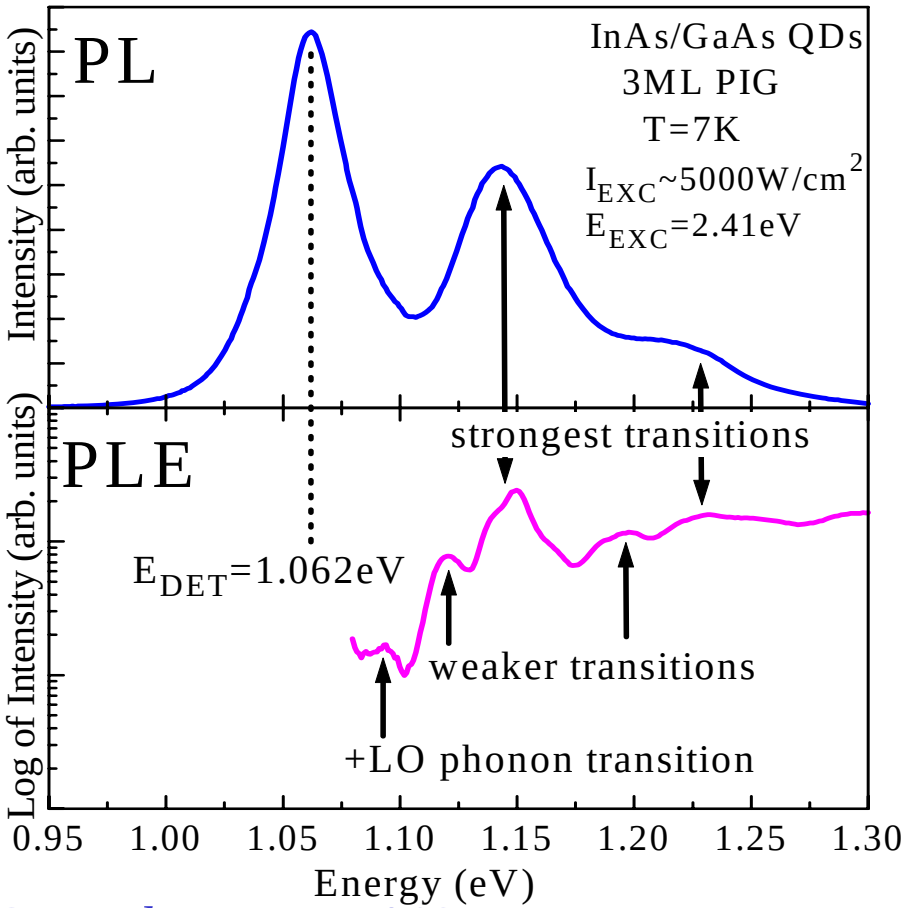

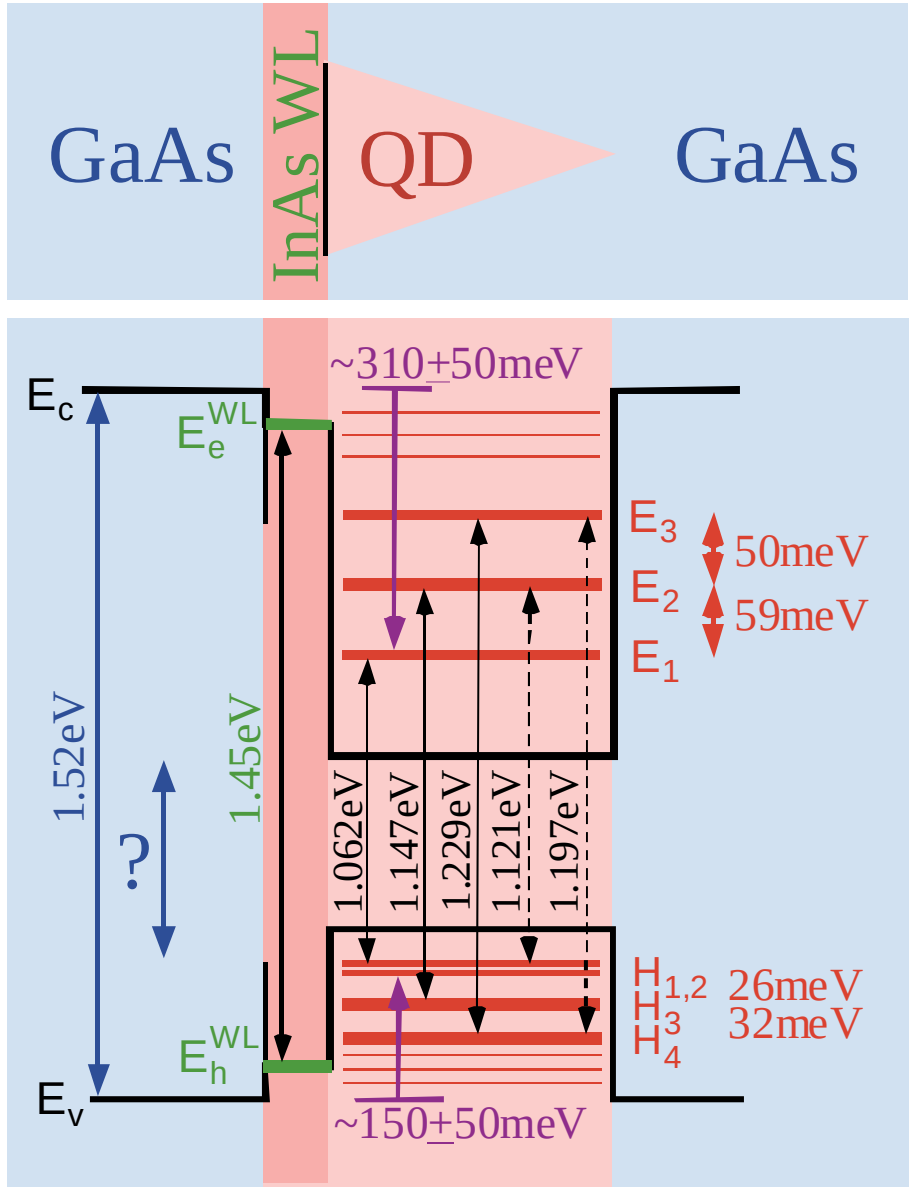

Ground state at 1.062eV

Excited states:

Strongest at 1.147eV and 1.229eV

Weaker at 1.121eV and 1.197eV

Intra-band Transitions

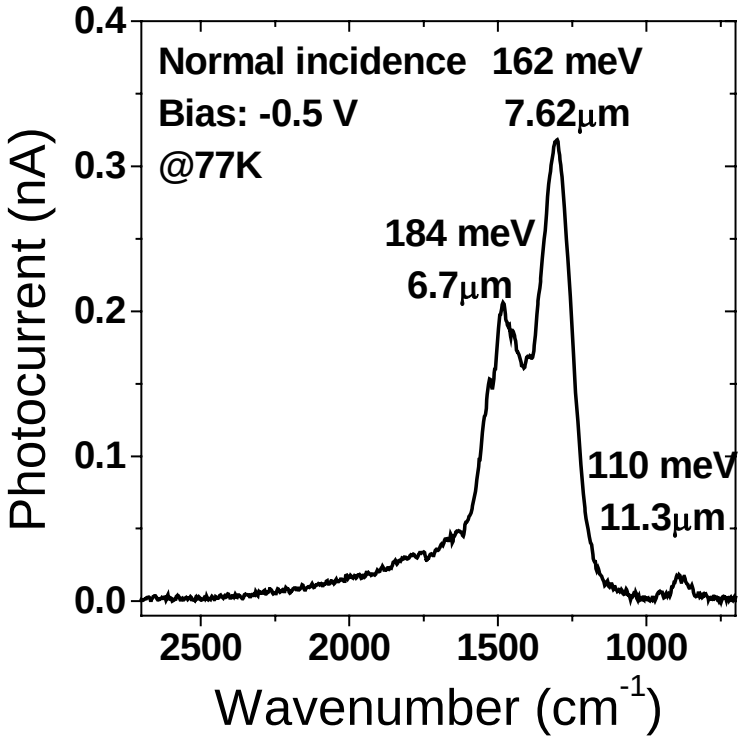

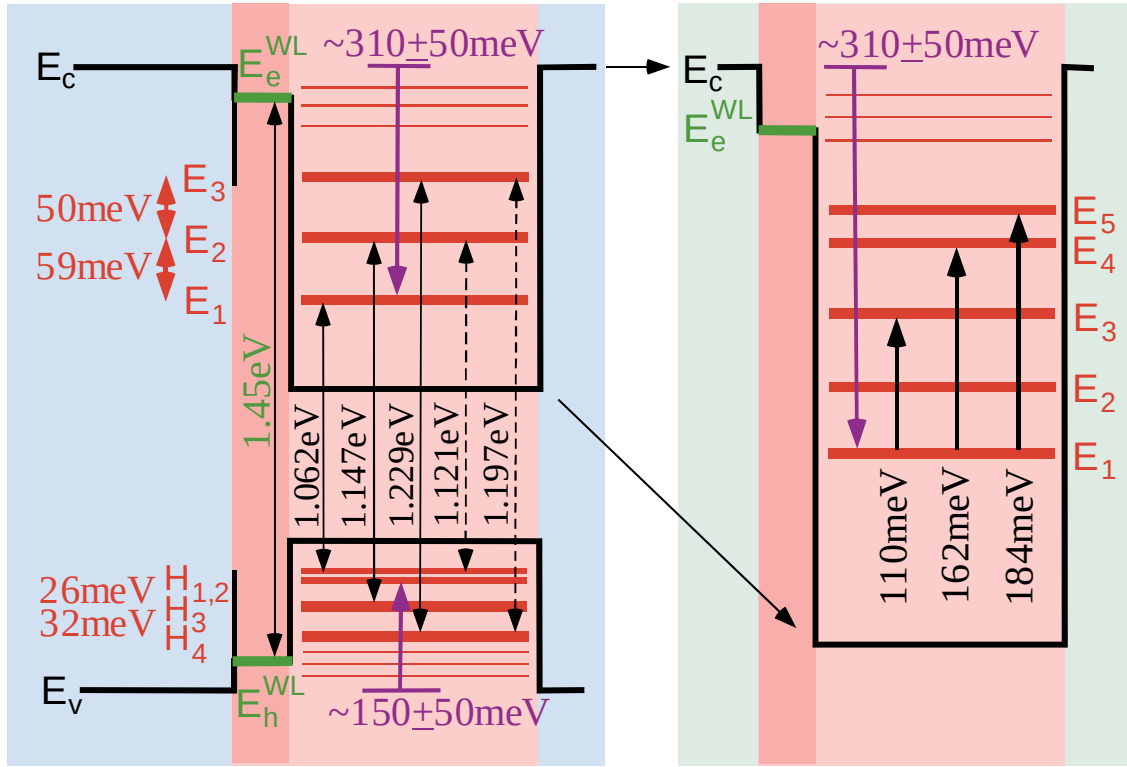

A. Madhkar (USC)

Intra-band Transitions

Table 4 Inter-sub band transition matrix elements of ground electron state to upper three electron states, $\left|\left\langle \phi_{1,c}|\bar{r}|\phi_{i,c}\right\rangle\right|^2$. B=200A, h=80A.

Symmetry	state i	x	y	z
A1	#2 (0.111)	0	0	0.2
	#3 (0.123)	0	0	57
	#4 (0.197)	0	0	201
A2	#2 (0.106)	0	0	28.5
	#3 (0.114)	0	0	0
B1,B2	#2 (0.109)	0	0	15
	#3 (0.138)	0	0	42
	#4 (0.201)	0	0	14
A1-B1n	#1 (0.062)	446	446	0
	#2 (0.162)	0.2	0.2	0
	#3 (0.218)	0.4	0.4	0
B1-A1n	#2(0.049)	536	536	0
	#3(0.061)	659	659	0
	#4(0.135)	376	376	0
	#5(0.161)	10.2	10.2	0

Single-electron transistor (SET)

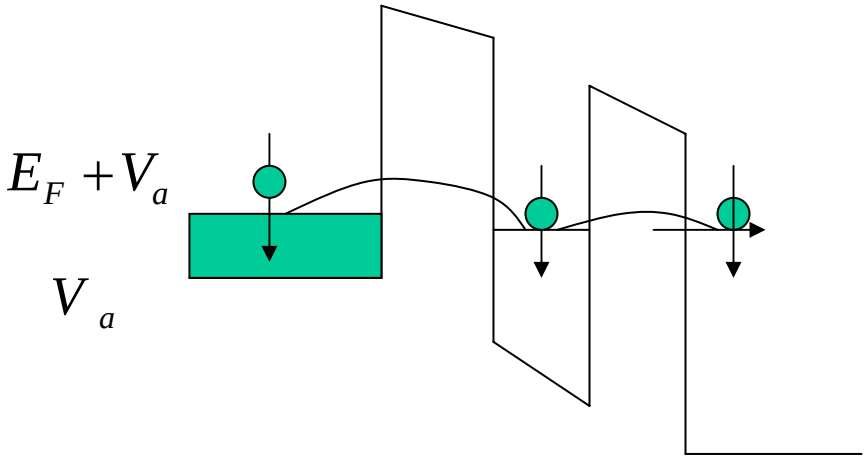

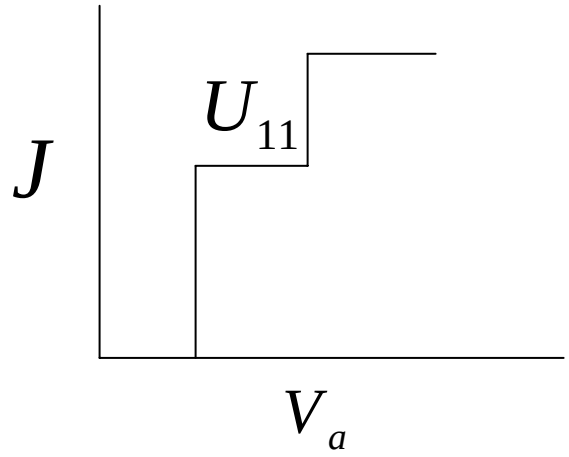

Coulomb blockade

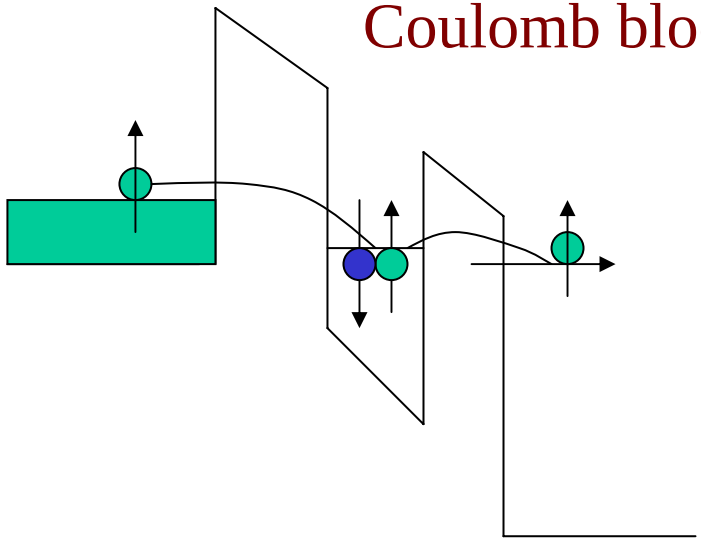

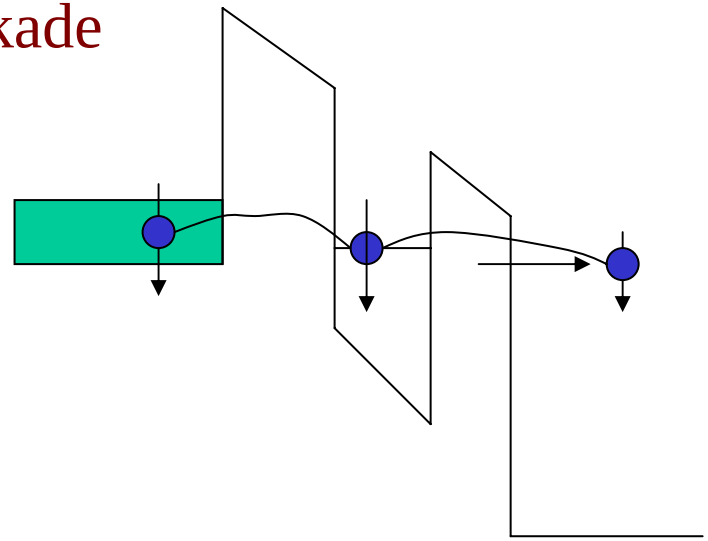

Tunneling current with Coulomb blockade

$$J = \frac{2e}{h}\sum_{\alpha}\int dw\Gamma[\, f_L(w-\mu_L) - f_R(w-\mu_R)]\,\mathrm{Im}\,G_{d\alpha}(w)$$

$$G_{d\alpha}(w) = [\frac{1-\langle n_{d,\alpha}\rangle}{w-\varepsilon_0+i\Gamma} + \frac{\langle n_{d,\alpha}\rangle}{w-\varepsilon_0-U\ \ +i\Gamma}]$$

$$\langle n_{d,-\alpha}\rangle = \langle n_{d,\alpha}\rangle = \frac{1}{\pi}\int_{-\infty}^{\infty} dw\,\frac{f_L(w-\mu_L)+ f_R(w-\mu_R)}{2}\,\mathrm{Im}\,G_{d\alpha}(w)$$

Effects of Coulomb blockade on the photocurrent in QDIPS

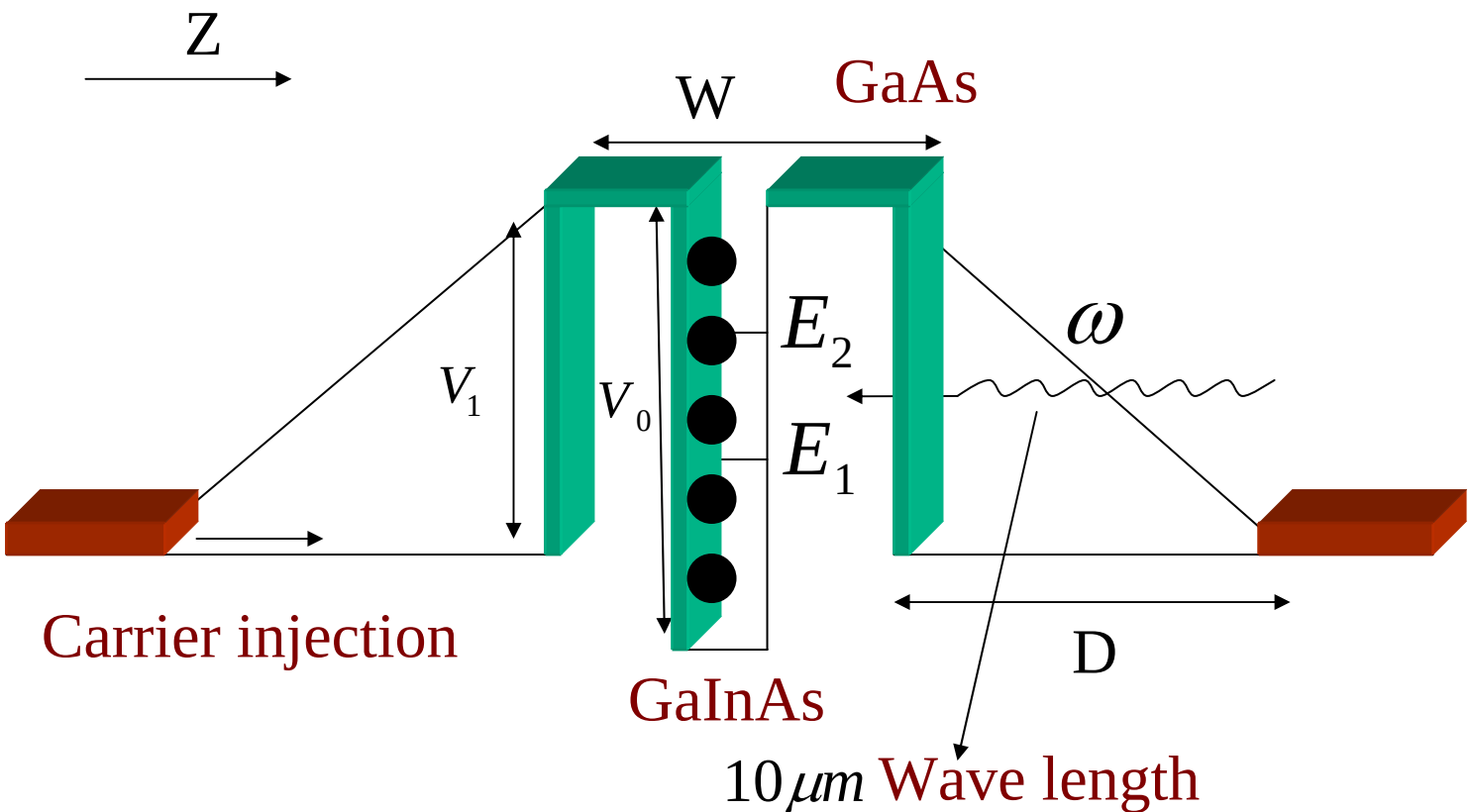

n-i-n structure

Atmospheric transmission windows 8-13 μm

Isolated system vs. open system

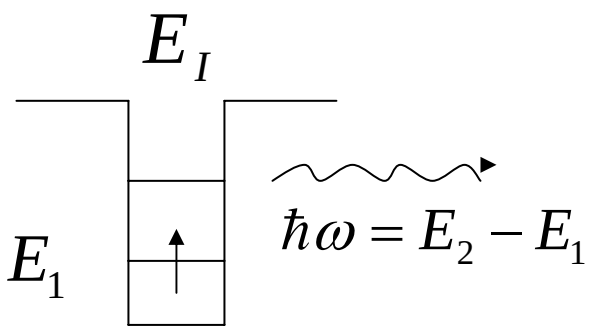

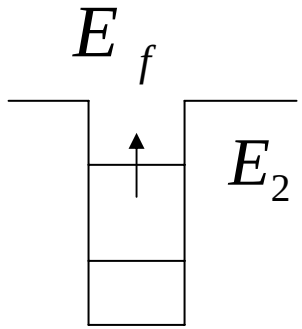

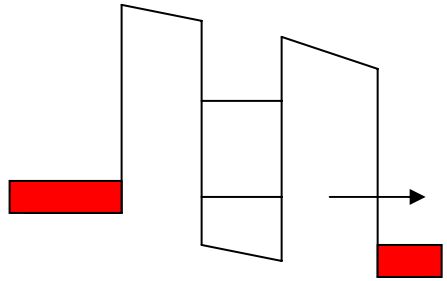

Red shift

Open system

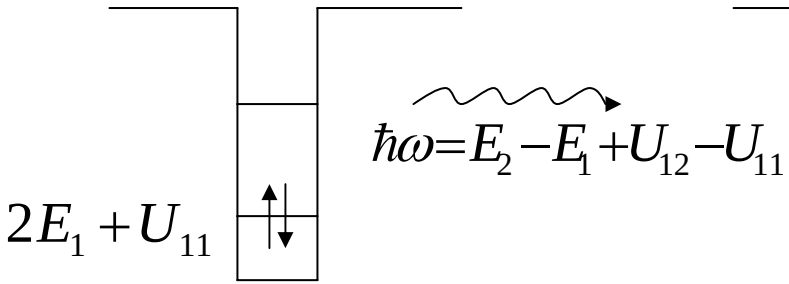

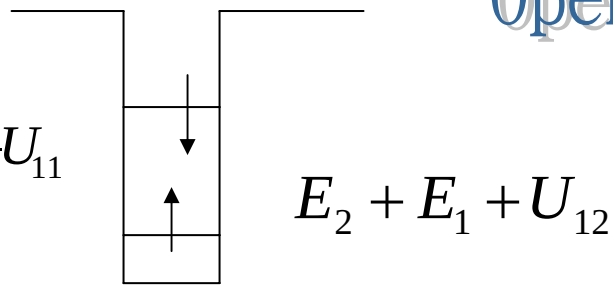

Photocurrent under various bias

$U_{11} = 11.34\ meV$

$U_{12} = 10.4\ meV$

Solid: $V_a = 0.11V$

Dashed: $V_a = 0.12V$

Dotted: $V_a = 0.13V$

Decaying = 0.1meV

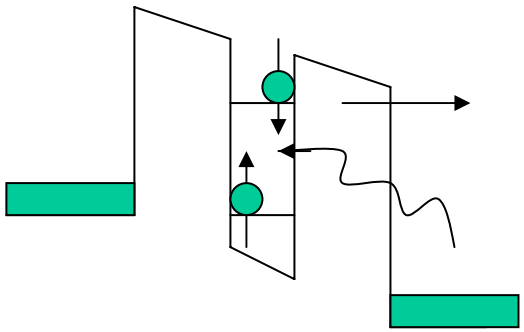

R=65A and h=50A

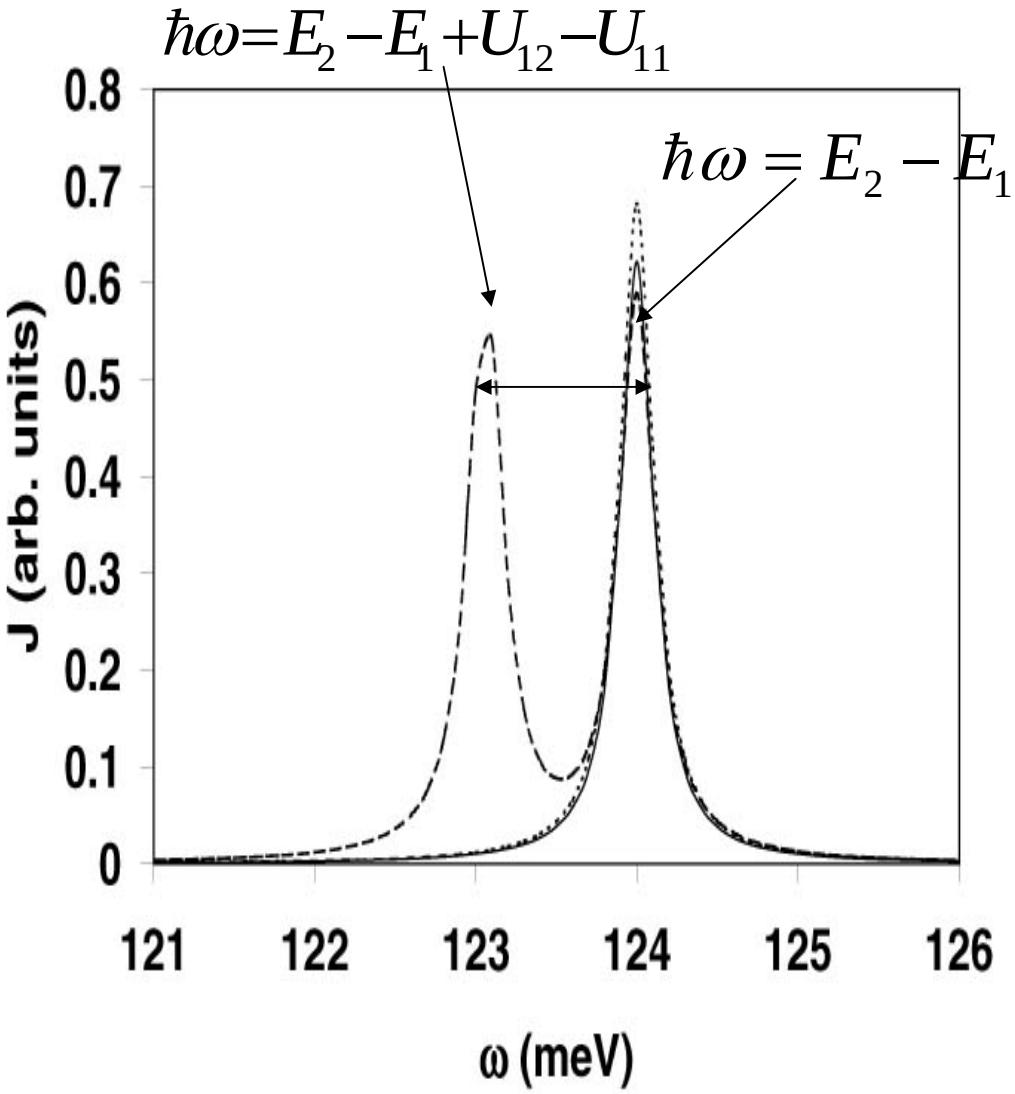

Single-Photon generator

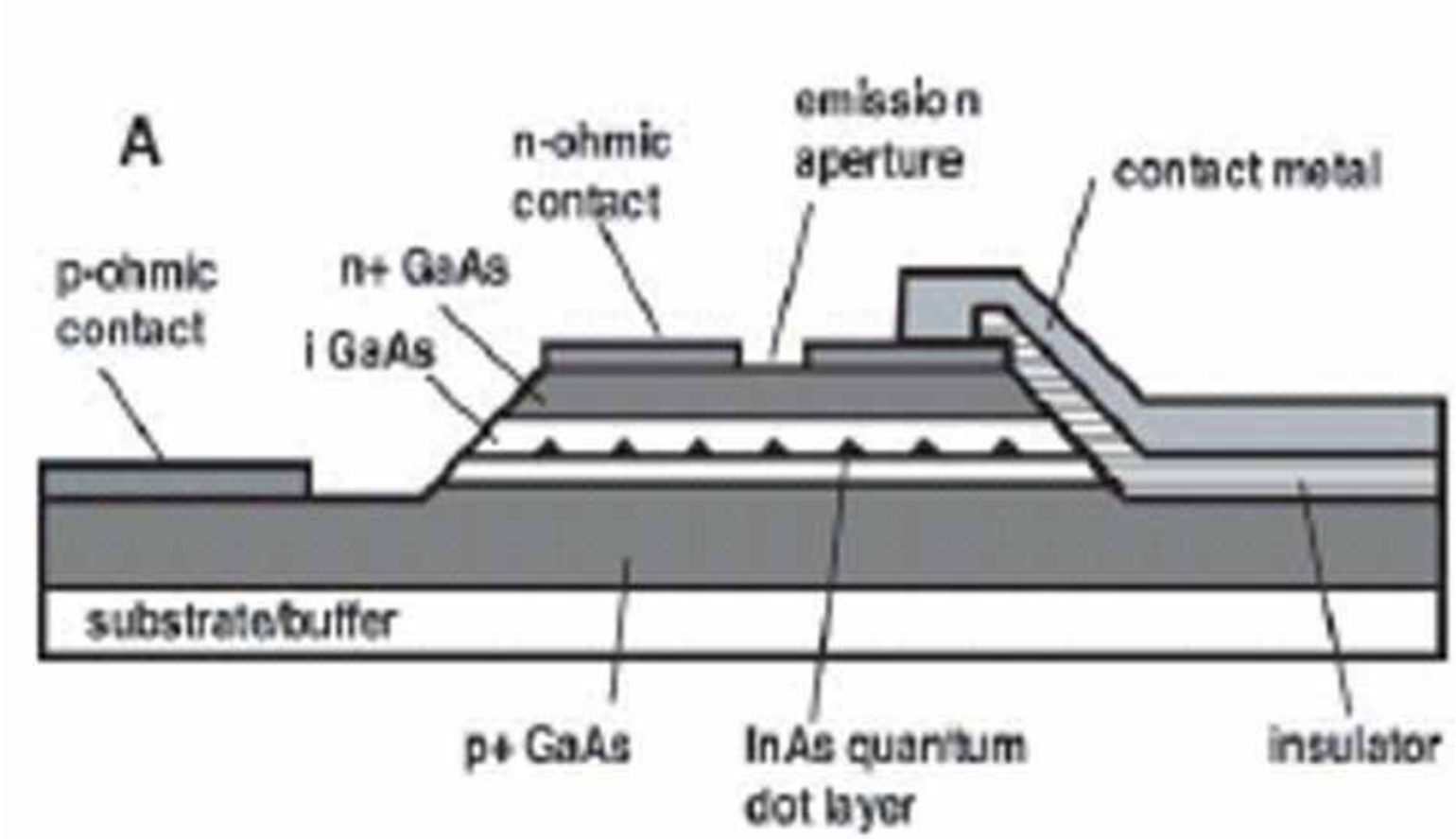

Z. Yuan et al., Science, 295, 102 (2002

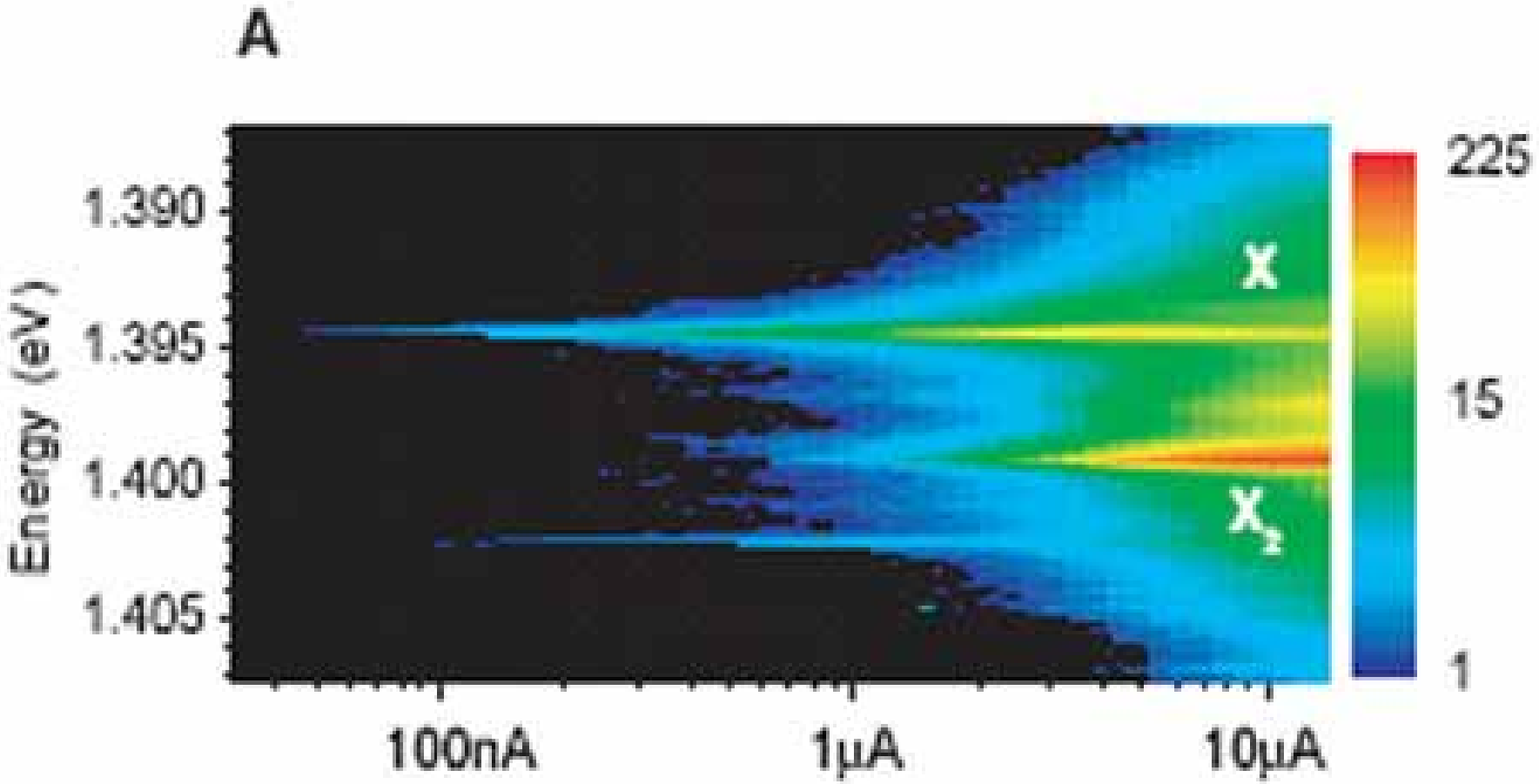

Z. Yuan et al., Science, 295, 102 (2002)

Keldysh Green Function

$$\Gamma_1 N_1 = -\mathrm{Im}p - \int \frac{d\varepsilon}{\pi} \Gamma_1^{L/R} f_{L/R}(\varepsilon) \mathrm{Im} G_{11}^r(\varepsilon + \frac{\omega}{2})$$

$$\Gamma_2 N_2 = \mathrm{Im}p - \int \frac{d\varepsilon}{\pi} \Gamma_2^{L/R} f_{L/R}(\varepsilon) \mathrm{Im} G_{22}^r(\varepsilon - \frac{\omega}{2})$$

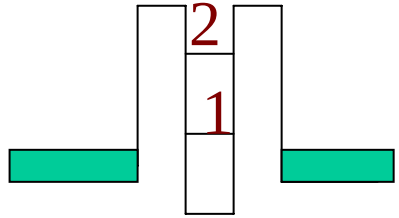

$$\mathrm{Im}p \approx 2\lambda^2 \int \frac{d\varepsilon}{2\pi} \frac{\Gamma_1^L f_L(\varepsilon) + \Gamma_1^R f_R(\varepsilon)}{\Gamma_1} \left\{ \mathrm{Im}\left(\frac{1 - N_1}{\varepsilon - E_1 + i\frac{\Gamma_1}{2}}\right) \mathrm{Im}\left(\frac{1}{\varepsilon - E_2 + \omega - i\frac{\Gamma_2}{2}}\right) \right.$$

$$\left. + \mathrm{Im}\left(\frac{N_1}{\varepsilon - E_1 - U_{11} + i\frac{\Gamma_1}{2}}\right) \mathrm{Im}\left(\frac{1}{\varepsilon - E_2 - U_{12} + \omega - i\frac{\Gamma_2}{2}}\right) \right\}$$

Coulomb interactions vs. QD size

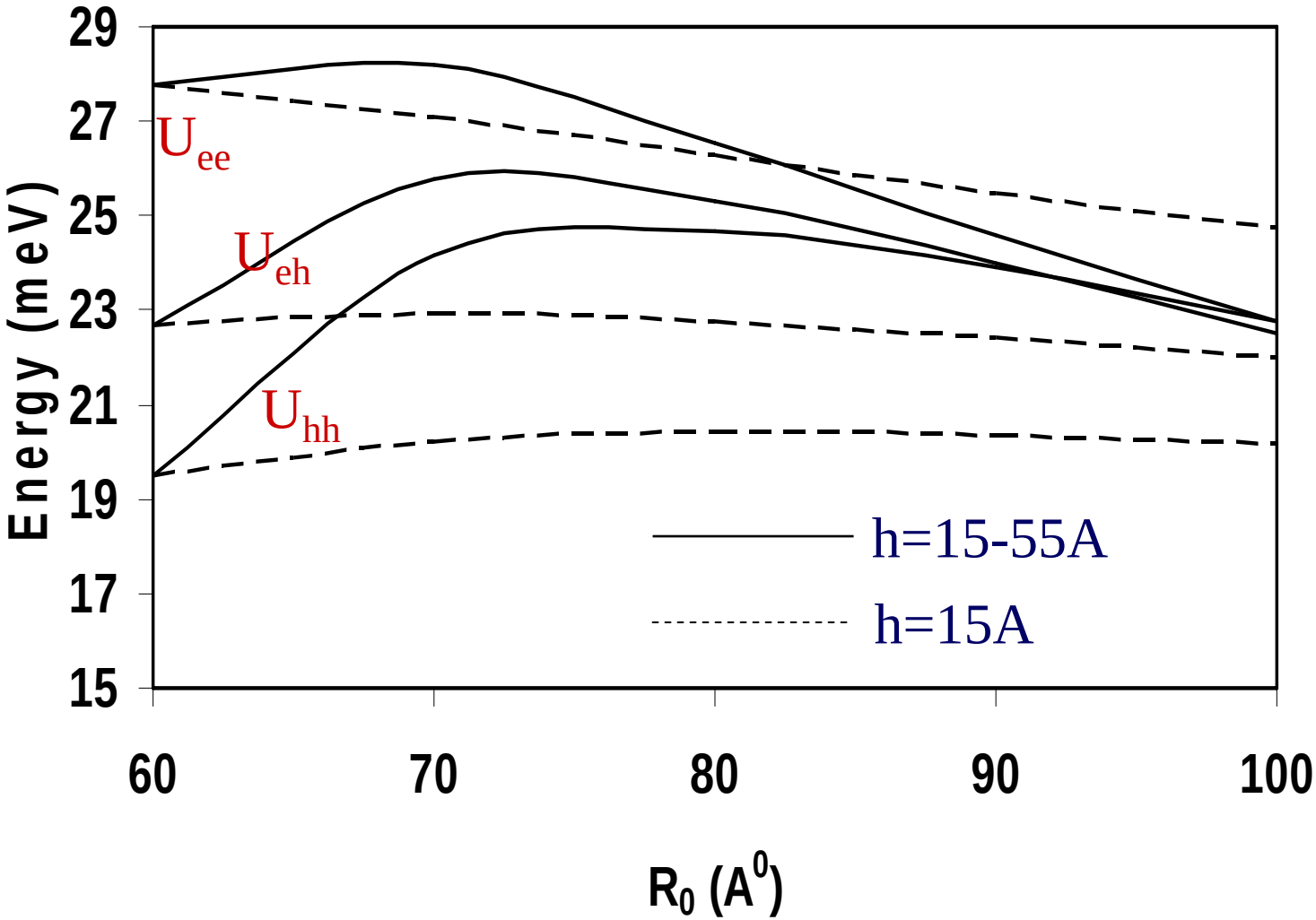

Spontaneous emission spectrum

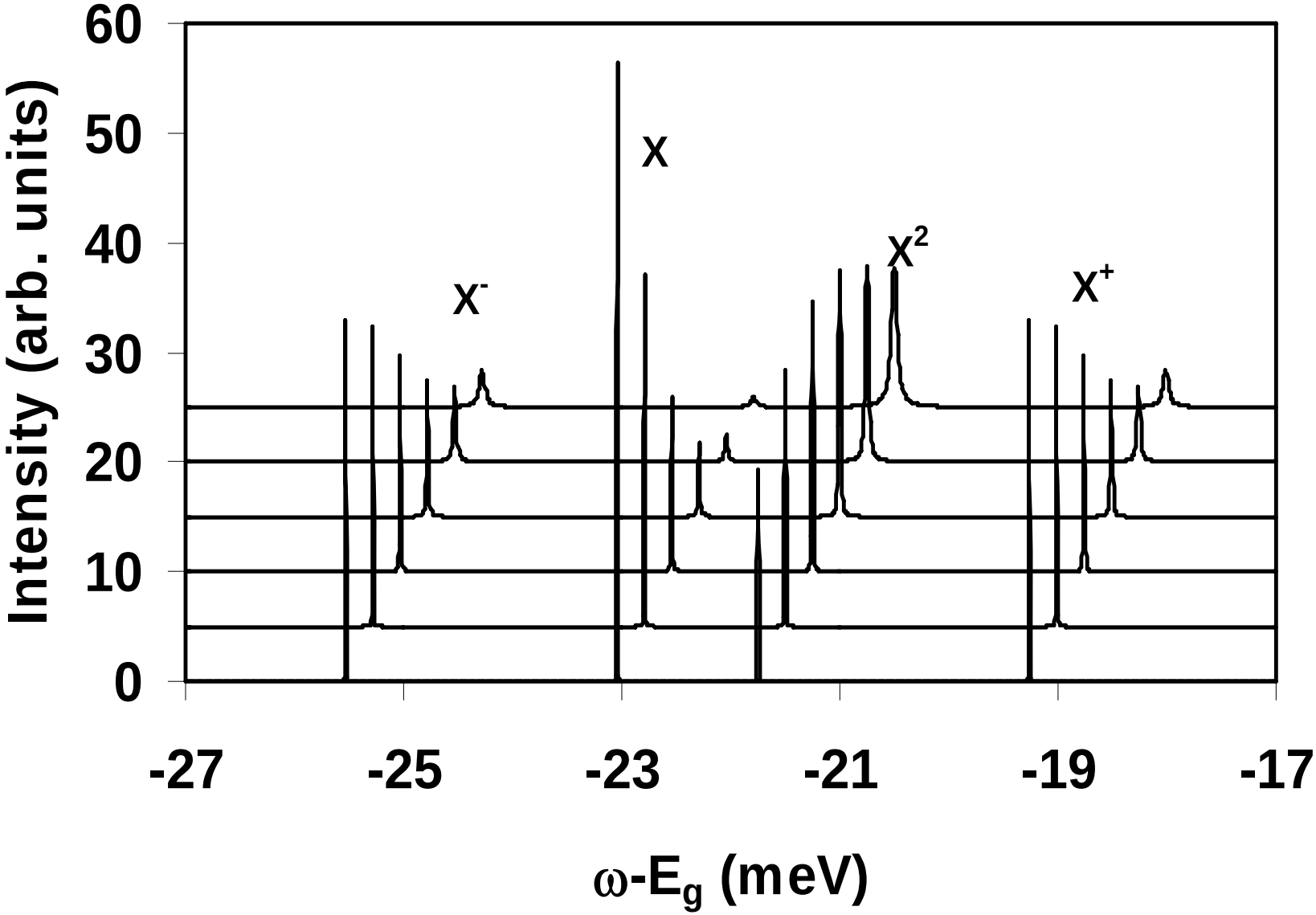

Intensity vs current

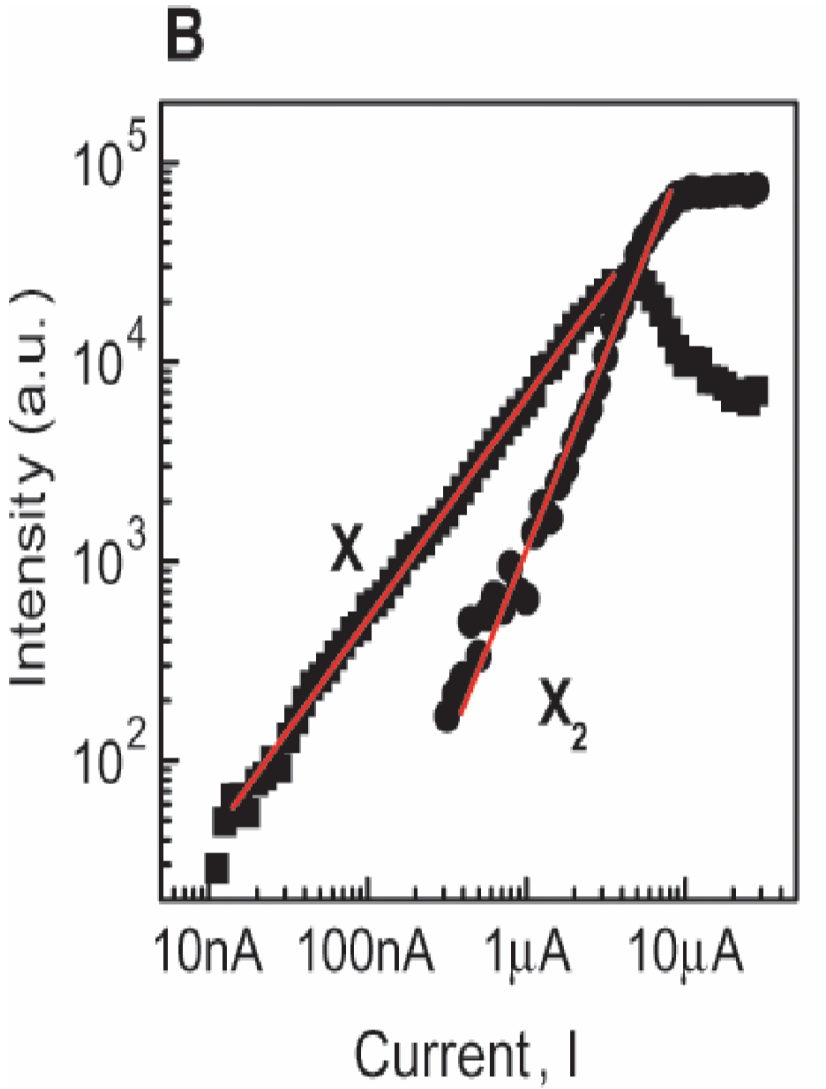

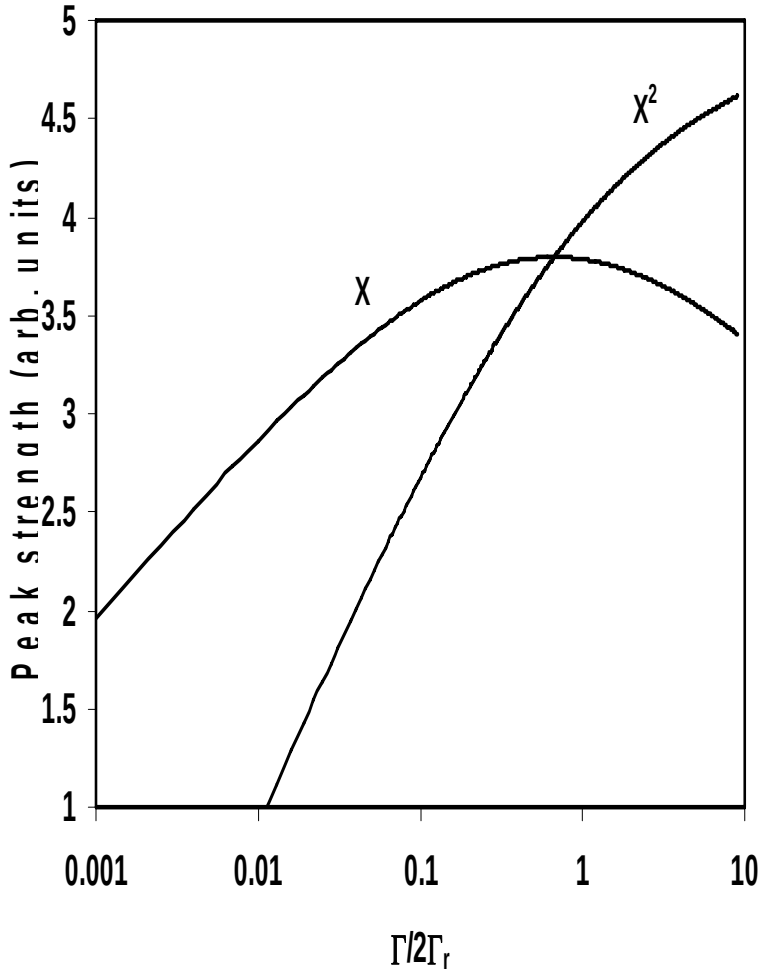

[Z. Yuan et al., Science, 295, 102 (2002)]

[Phys. Rev. B **69**, R41306 (2004)]

Tunneling current spectroscopy of a nanostructure junction involving multiple energy levels

David M T Kuo & Y. C. Chang

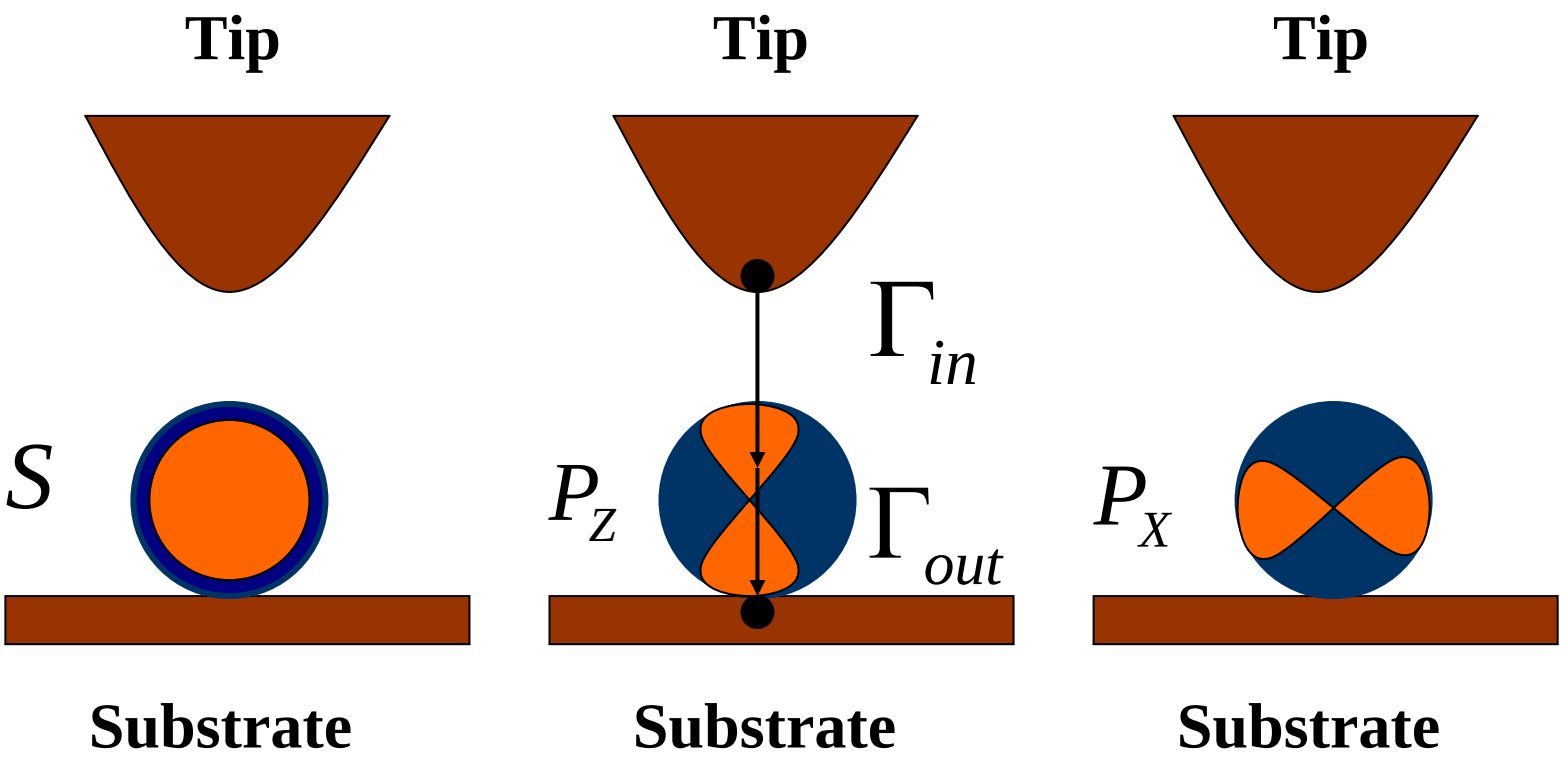

E_s, E_{p_z}, E_d

P. Liljeroth et al, Phys. Chem.chem. Phys. 8, 3845 (2006)

2.1 Shell-tunneling and shell-filling

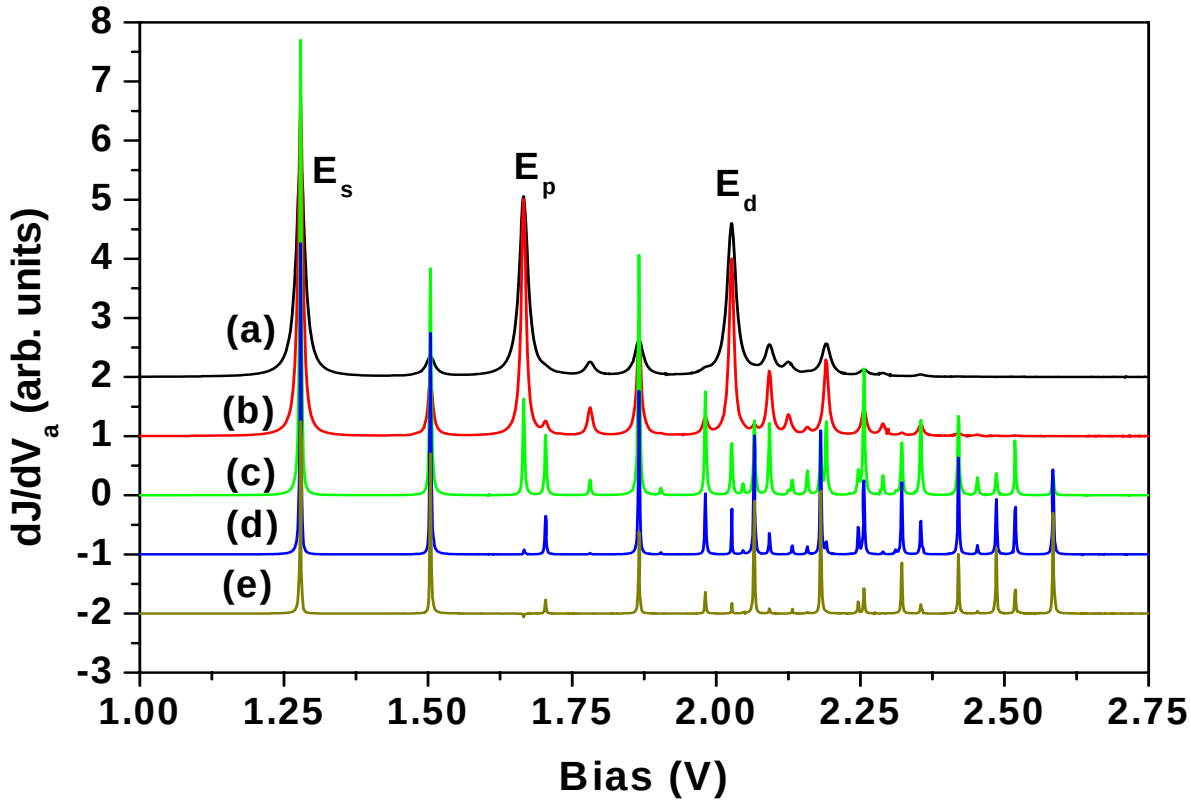

Theoretical vs. Experimental results for STM-QD tunneling spectra

[L. Jdira et al., Phys. Rev. B 73, 115305 (2006)]

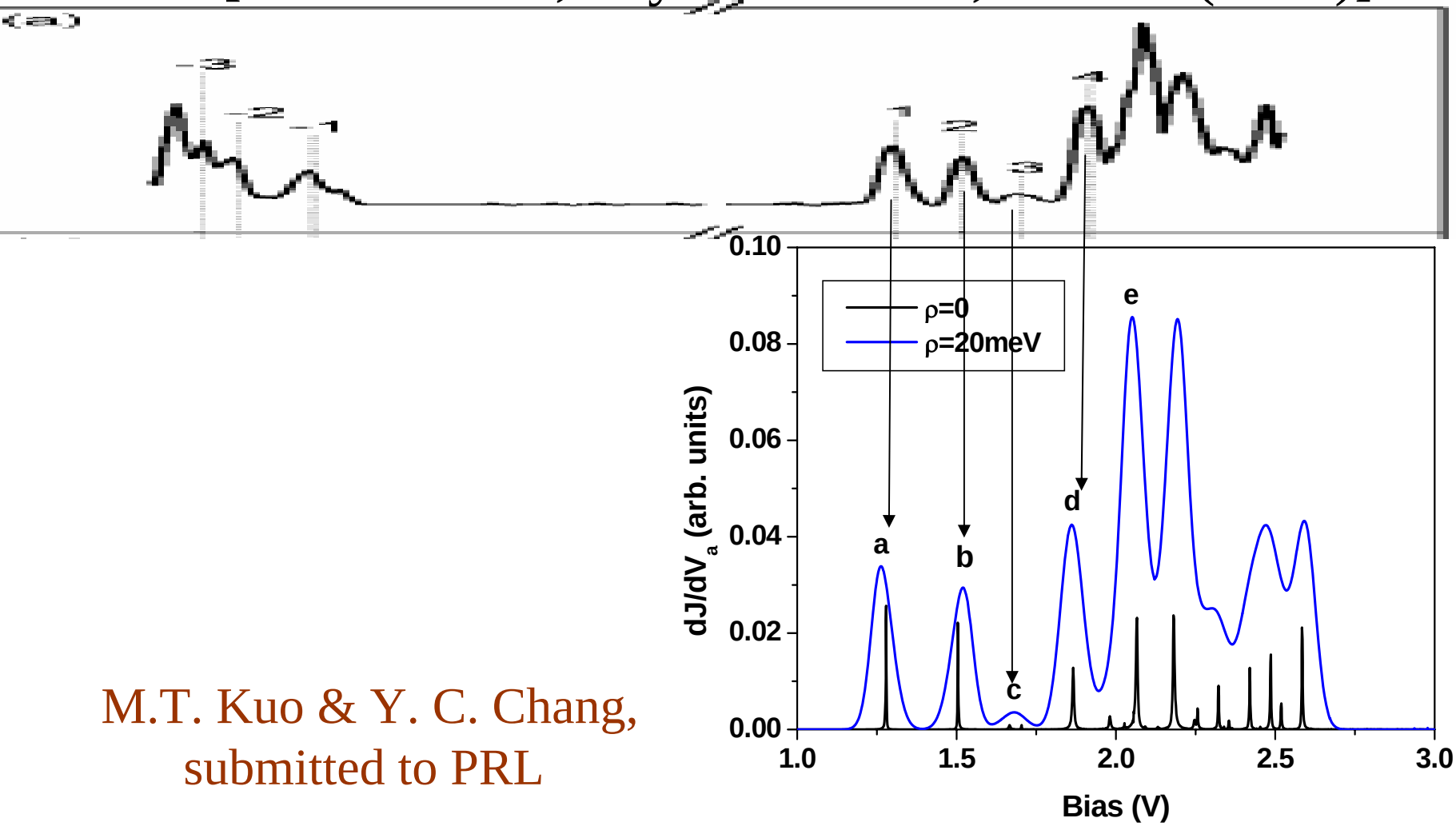

M.T. Kuo & Y. C. Chang, submitted to PRL

2.4 Differential conductance at negative bias

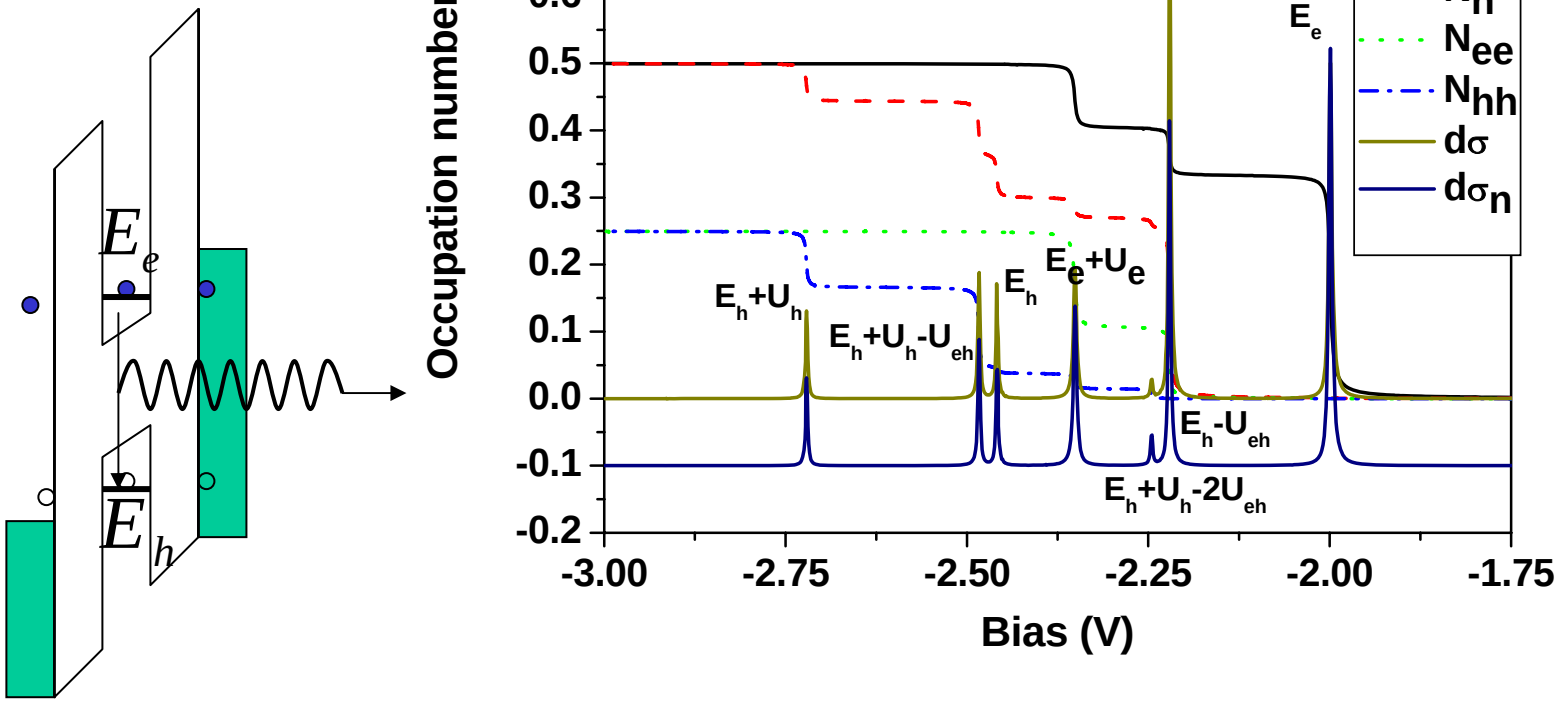

Negative differential conductance in coupled QDs

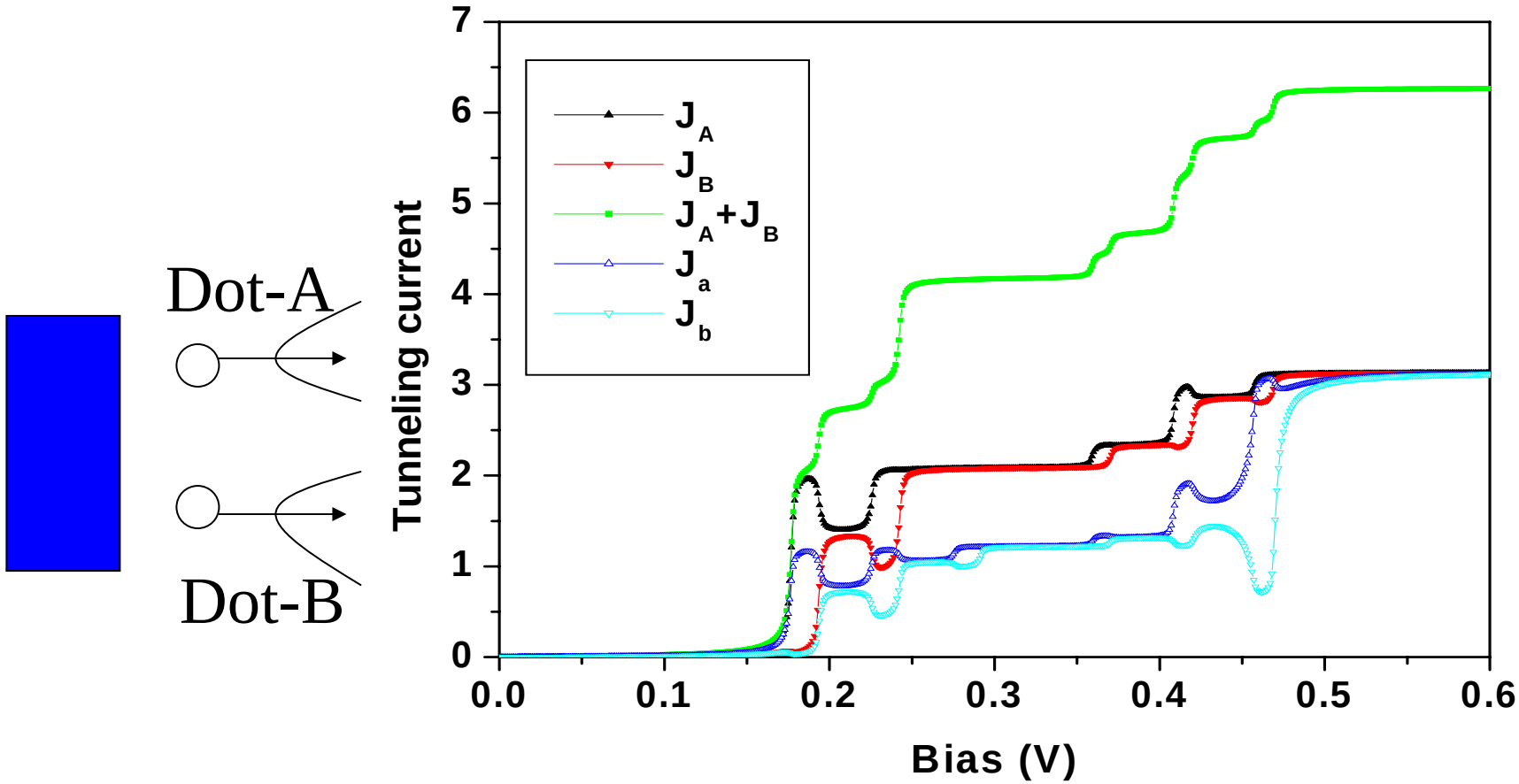

Proximity effect for tunneling current in nanojunction with coupled QDs

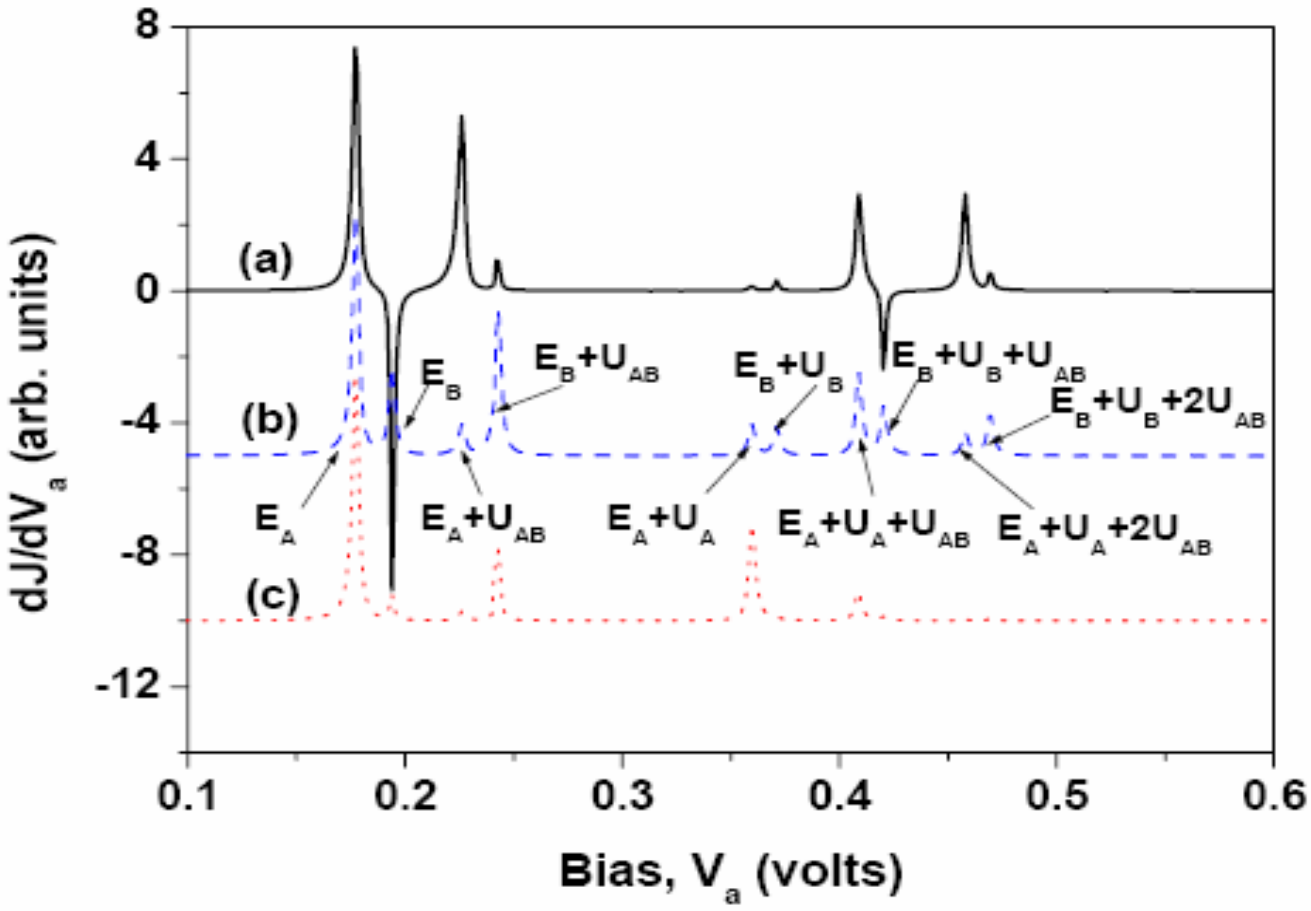

FIG. 4: Differential conductance as a function of applied bias for various tunneling rate ratios of $\Gamma_{L,B}/\Gamma_{R,B}$. $U_{AB} = 30$ meV. (a) $\Gamma_{L,B} = 1$ meV and $\Gamma_{R,B} = 0.1$ meV. (b) $\Gamma_{L,B} = 1$ meV and $\Gamma_{R,B} = 1$ meV. (c) $\Gamma_{L,B} = 0.1$ meV and $\Gamma_{R,B} = 1$ meV.

Summary

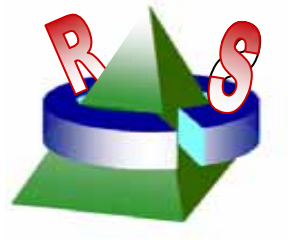

- SAQDs can be suitably modeled by VFF+EBOM
- EMA can produce realistic predictions by choosing proper model potentials
- Intra-level and inter-level Coulomb interactions play keys roles in the optical properties
- . Multiple-peak structures coexist for a single QD under bias (Open system) in photocurrent and emission spectra
- . Coulomb blockade can lead to negative differential photo-conductance
- Non-equilibrium transport and correlation are important in the analysis of single-photon detector/generator